Prediction of Geomechanical Properties and Seismic Inversion Analysis of Khipro Area, Thar Platform, Pakistan

By

ABDUL BASIT

M.Phil Geophysics

Department of Earth Sciences

Quaid-i-Azam University

Islamabad, Pakistan.

2019

CERTIFICATE

This dissertation submitted by ABDUL BASIT S/O MUHAMMAD SAEED is accepted in its present form by the Department of Earth Sciences, Quaid-I-Azam University Islamabad as satisfying the requirement for the award of M.Phil. in Geophysics.

RECOMMENDED BY

Dr. M Gulraiz Akhter _____

(Supervisor & Chairman Department of Earth Sciences)

External Examiner _____

ACKNOWLEDGEMENT

Starting from the name of Allah, the most Beneficent, the most Merciful. All praises to Almighty Allah, the creator of universe. I bear witness that there is no God but Allah and Holy Prophet Hazrat Muhammad (P.B.U.H) is the last messenger of Allah, whose life is a perfect model for the whole mankind till the Day of Judgment. Allah blessed me with knowledge related to Earth. Without the blessing of Allah, I could not be able to complete my work as well as to be at such a place.

I am indebted to my friends, family and colleagues especially to my dissertation supervisor Dr. Muhammad Gulraiz Akhter for giving me an initiative to this study. His inspiring guidance, dynamic supervision and constructive criticism, helped me to complete this work on time. Heartily thanks to whole faculty of Department of Earth Sciences. Special thanks to Maarij Ahmed Siddiqui whose valuable knowledge, assistance, cooperation and guidance throughout my studies enabled me to take initiative, develop and furnish my academic career. I would like to thanks all my friends who helped me in studies and supported me with constant motivation and last but not the least my parents and my family's continuous support and encouragement played a vital role in my life. I am nothing without them.

ABDUL BASIT

DEDICATION

This work is dedicated to my siblings and parents, I am who I am because of them.

Abstract

Khipro field is an important producing field of Pakistan; geographically situated in district Sanghar in Sindh and geologically positioned in Lower Indus Basin. To find trapping mechanism formed by normal faults, seismic interpretation is carried out in fractured reservoir of Cretaceous age. Horst and Grabens are recognized in this field. To typify reservoir quality, Petrophysical evaluation have been employed. Results are up to the mark for reservoir zone i.e. Basal Sand with medium to low shale volumes possessing high values of effective porosity and low water saturation. Seismic inversion aimed to extrapolate the quantified inverted parameters beyond the vicinity of well point. Post stack inversion techniques are used to verify the interpretation reliability, reservoir quantification and pore pressure estimation. Post stack inversion algorithms of Sparse spike and Model based are implemented to see their relative outputs. Well stability during Borehole drilling costs 8$ billion roughly in oil and gas sector worldwide. Therefore an evaluation of formation pressure and fracture gradient before drilling an exploratory well, help oil companies to handle their capital resources in a better way. Pore pressure prediction is an important tool contributes in risk analysis before discovering hydrocarbons. Estimating pore pressure in formation helps all shareholders to design a better strategy which ensure well control during exploration activities. The dissertation focuses on prediction of pore pressure, overpressure and under-pressure by applying Eaton's and Bowers methods using log data of Khipro boreholes and extrapolating these estimates on seismic section using inverted parameters. Some over-pressured zones are found in wells Naimat-Basal-01 and Siraj-south-01 whereas mostly normal pressure prevailed in the study area. In situ stresses formed the basis for unconventional reservoir.

Table of Contents

CHAPTER 1 1
INTRODUCTION 1
1.1 Overview 1
1.2 Location and Physiography 1
1.3 Exploration History 2
1.4 Data Base 3
1.5 Motivation and Research Objectives 4
1.6 Methodology 5
CHAPTER 2 6
GENERAL GEOLOGY 6
2.1 Sedimentary Basins 6
2.2 Basins of Pakistan 6
2.3 Structural Settings of Southern Indus Basin (Study Area) 6
2.4 Regional Stratigraphy 9
2.5 Stratigraphic Sequence of Khipro Area 9
2.6 Petroleum Play of The Study Area 9
2.6.1 Source Rock 9
2.6.2 Reservoir Rock 9
2.6.3 Cap Rocks 10
CHAPTER 3 12
SEISMIC DATA INTERPRETATION 12
3.1 Introduction 12
3.2 Structural Interpretation 12
3.3 Stratigraphic Interpretation 12
3.4 Workflow for Interpreting Seismic Data 12
3.5 Identification of Seismic Horizons 13
3.6 Generation of Synthetic Seismogram 14
3.7 Marked Seismic Sections 14
3.8 Constructing Fault Polygon 17
3.9 Contour Maps 17
3.9.1 Time Contour Maps 18

3.9.2 Depth Contour Maps 18
CHAPTER 4 21
WELL LOG ANALYSIS 21
4.1 Introduction 21
4.2 Scheme for Log Analysis 22
4.2.1 Quantifying Clay 22
4.2.2 Quantifying Shale 22
4.2.3 Porosity Computation 22
4.3 Petrophysical Analysis of Naimat Basal-01 and Siraj South-01 24
CHAPTER 5 29
POST STACK SEISMIC INVERSION 29
5.1 Introduction to Seismic Inversion 29
5.2 Types of Seismic Inversion (Post Stack) 31
5.2.1 Model Based Inversion 31
(a) Extracting Wavelet 32
(b) Well to Seismic Tie 33
(c) Initial Model With Low Frequency 34
(d) Inversion Analysis 35
5.2.2 Sparse Spike Inversion 37
5.3 Comparison of Model Based and Sparse Spike Inversion: 39
CHAPTER 6 41
PORE PRESSURE PREDICTION USING WELL DATA 41
6.1 Introduction to Pore Pressure 41
6.2 Hydrostatic Pressure 41
6.3 Overburden Pressure 42
6.4 Pore Pressure (Pp) 42
6.5 Normal, Over and Under Pressure 43
6.6 Vertical Effective Stress 43
6.7 Pore Pressure Prediction 43
6.8 The Normal Compaction Trend (NCT) 43
6.9 Disequilibrium Compaction 45
6.10 Pore Pressure Prediction Methods 45
6.10.1 Eaton Ratio Method 46

6.10.2 Bowers Method 47
6.11 Pore Pressure Prediction Workflow From Well Log Data 47
6.12 Well Based Pore Pressure Prediction 48
6.13 Results and Analysis: 48
6.13.1 Low Pressure Generation Mechanism 51
6.13.2 Overpressure Generating Mechanism 52
6.14 Estimation of Pore Pressure 52
6.15 Magnitude of In Situ Stresses 55
6.15.1 Vertical Stress 55
6.15.2 Minimum Horizontal Stress 56
6.15.3 Fracture Pressure and Closure Stress 57
6.15.4 Maximum Horizontal Stress 58
Conclusions 62
References 63

List of Figures

Figure 1.1 Geographic location of study area (Banks and Warburton, 1986). 2
Figure 1.2 Base map of the area under study. 4
Figure 1.3 Methodology adopted for dissertation. 5
Figure 2.1 Basin architecture of the lower part of Indus Basin (Khan et al., 1986). 8
Figure 2.2 Tectonic scheme of Pakistan (Kazmi and Snee, 1989). 8
Figure 2.3 Stratigraphic Succession of lower part of Indus Basin (Khan et al., 1986). 11
Figure 3.1 Workflow for seismic data interpretation. 13
Figure 3.2 Synthetic seismogram of Naimat basal-01. 14
Figure 3.3 Interpreted time section for line 2000KH-08. 15
Figure 3.4 Interpreted time section for line 2000KH-30. 15
Figure 3.5 Marked seismic section for line2003KH-35. 16
Figure 3.6 Marked seismic section for line2003KH-44. 16
Figure 3.7 Fault polygon at Lower Goru horizon. 17
Figure 3.8 Fault polygon at Basal sand horizon. 18
Figure 3.9 Time contour map at Lower Goru horizon. 19
Figure 3.10 Time contour map at Basal sand horizon. 19
Figure 3.11 Depth contour map at Lower Goru horizon. 20
Figure 3.12 Depth contour map at Basal Sand horizon. 20
Figure 4.1 Workflow followed for the petrophysical analysis. 21
Figure 4.2 Well Logs of Naimat Basal 01. 25
Figure 4.3 Well Logs of Siraj South 01. 27
Figure 5.1 Work flow of seismic inversion (Veeken and Silva, 2004). 30
Figure 5.2 Steps adopted for post stack seismic inversion (Sen and Stoffa, 1995). 30
Figure 5.3 Subdivision of acoustic impedance inversion (Veeken and Silva, 2004). 31
Figure 5.4 Model base inversion workflow for estimating acoustic impedance, porosity and lithology (Kneller at al., 2013). 32
Figure 5.5 Extracted statistical wavelet showing amplitude and phase spectra from seismic 33
Figure 5.6 Well to seismic tie at well Naimat-Basal-01. 34
Figure 5.7 Initial Model having Low frequency. 35
Figure 5.8 Post Stack Seismic inversion analyses (Model based) at Naimat-Basal-01 36
Figure 5.9 (a) Cross sectional view of Low impedance zone of line 2000KH-08 36
Figure 5.9 (b) Cross sectional view of inverted impedance of line 2000KH -08 37
Figure 5.10 Results of Sparse Spike inversion analysis. 38
Figure 5.11 Inverted section of line 2000KH-08 at Naimat-Basal-01. 39
Figure 5.12 Model based inversion 40

Figure 5.13 Sparse Spike inversion……40

Figure 6.1 Basic terminologies used in Pore Pressure (Nwankwo, C.N. and Kalu, S.O. 2016)……42

Figure 6.2 (a) Normally pressured sediments gradient will lies on hydrostatic profile in pressure depth profile (b) Porosity decreases with depth for normally compacted sediments in a predictable manner (c) Normal compacted sediments produces a straight line in porosity effective stress profile (Swarbrick, 2012). 44

Figure 6.3 Generalized Workflow of Pore Pressure Prediction from Well logs data. 47

Figure 6.4 Pore pressure prediction sequence for Naimat-Basal-01 well. 49

Figure 6.5 Over pressured shale sequence of upper Goru formation in Naimat-Basal-01 well. 50

Figure 6.6 Pore pressure prediction sequence for Siraj-South-01 well. 51

Figure 6.7 Cross Plots between Density and velocity for Naimat-Basal-01(left) and Siraj-South-01(right) wells, along the regression line data points showing the pressure due to disequilibiruim and the diversified points are indicating the pressure generated due to other mechanisms such as diagenesis of clay or expansion of fluid. 52

Figure 6.8 (a) Training Result of Multiple Attribute Regression Analysis (b) Training result of probabilistic neural network. 54

Figure 6.9 Cross-plot of actual and predicted porosity. 55

Figure 6.10 Extrapolation of predicted pore pressures for Naimat-Basal-01well on seismic line 2003KH-08 using seismic. 56

Figure 6.11 Fracture gradient or minimum horizontal stress along with maximum horizontal stress for Naimat-Basal-01 well. 58

Figure 6.12 Fracture gradient or minimum horizontal stress along with maximum horizontal stress for Siraj-South-01 well. 60

List of Tables

Table 1.1: Seismic data used for research work. 3
Table 1.2: Well log data.....3
Table 2.1. Stratigraphy of the study area. 10
Table 4.1: Calculated Petrophysical Parameters for Naimat Basal-01. 28
Table 4.2: Calculated Petrophysical Parameters for Siraj-South-01.....28
Table 6.1 List of Multiple Attributes with training errors. 53

CHAPTER 1

INTRODUCTION

1.1 Overview

For a long seismic data has been and is being used to demarcate the geometry of subsurface reflector and to determine their depth. However, seismic data contains profound knowledge more than reflection depth. Hydrocarbon accumulation is likely illuminated in the reflection of seismic wave. In every reflection, the amplitude of returned wave is different. Contrarily this is true because seismic wave reflect their amplitude, changes reveal significant material about the underlying material. The factor which is controlling these changes is contrast in impedance.

The quantitative use of seismic amplitude for the reservoir properties has acquired eminence lately. Consequently the amplitude in seismic reflection can be used to turn back or revert impedance by using the state or art of seismic inversion, when calibrated with well data can be accustomed to extract details such as lithology, saturation, porosity and geo-mechanical properties which help to bridge up the gaps in inter-well regions.

The beginning for all geo-mechanical analysis is a brief perception of the subsurface stress state, pore pressure and the mechanical properties which as a whole can be termed as geo-mechanical or mechanical model of earth. Geo-mechanics has owed different meanings for different people in oilfield. However, majority of the authors agree when subjected to geo-mechanics that it is the study of stress and strain, its magnitude and direction and its effect upon the rocks in a region for well bore stability analysis (Zoback, 2007; Wikel, 2011). Commonly it's a broader discipline including the use of seismic data along with well log response to perform relative analysis of pore pressure, stress and magnitude and mechanical earth properties constraints by local geology using seismic data.

1.2 Location and Physiography

Khipro (25º20'N-26º30'N and 68º20'E-69º14'E) is the study area which is an administrative subdivision of Sanghar district. Sited in the southern side of Pakistan and is a segment of Lower Indus Basin. Jacobabad High isolates the Lower Indus Basin from Central Indus

Basin. This area lies in extensional regime therefore normal faults prevail in the area. The location map about concerned region is displayed in Figure 1.1.

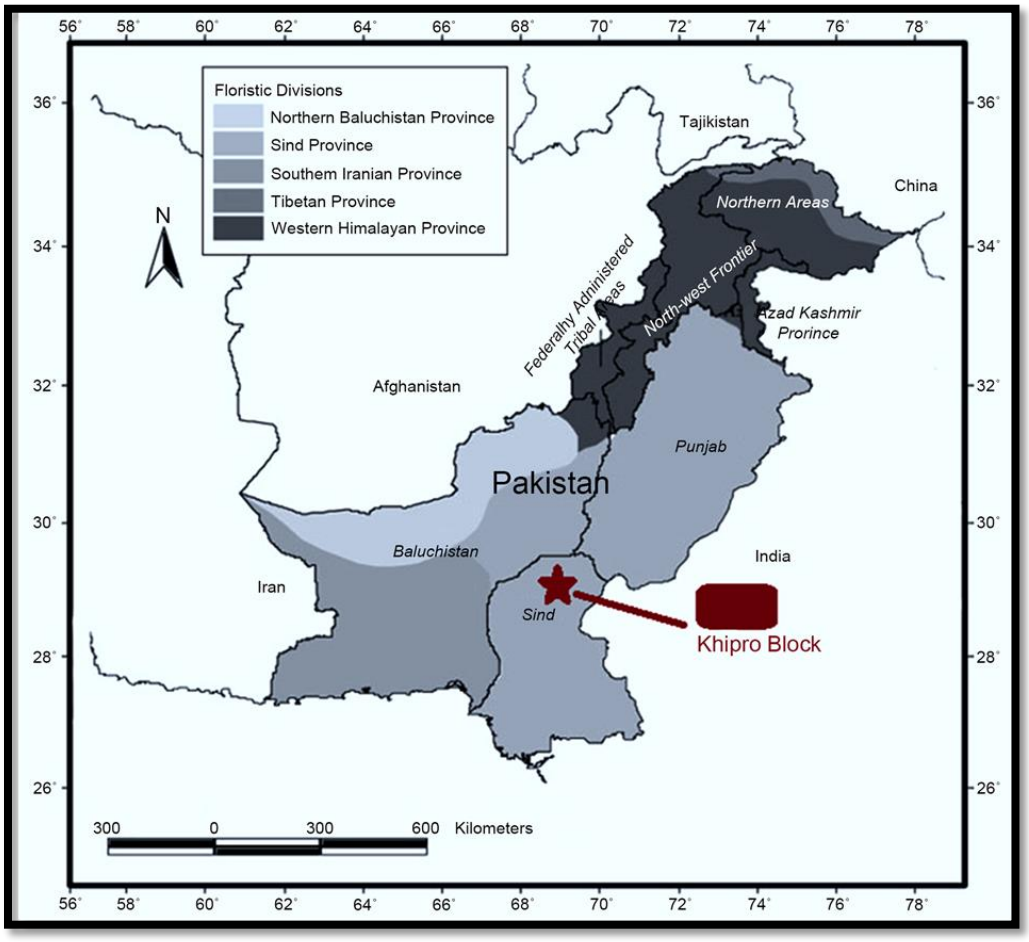

Figure 1.1 Geographic location of study area (Banks and Warburton, 1986).

1.3 Exploration History

As an operator Orient petroleum international Inc. (OPII), they made six discoveries from the fourteen exploratory wells which they drilled uptil now in this area. These six are Naimat-Basal-01 with starting rate of (27 million cubic feet per day (MMscfd)), Bilal North-01 (6 MMcfd), Bilal-01 (14.5 MMscfd), Siraj South-01 (24.3 MMscfd), Kamal North (2070 barrel oil per day (BOPD)) and Rahim-01 (825 BOPD) are included. Khipro's operator ship has been shifted to British Petroleum (BP) from January 2009 including its entire working interest by OPPII after fulfilling the commitment under the Production Companies Association (PCA) work program

(OPII annual report, 2009). In September 2011, United Energy Pakistan Limited (UEPL) took the charge of Khipro block from BP and planned to acquire 3D seismic data.

1.4 Data Base

The information accessible to accomplish this work spans over 14 lines along with four wells. Seismic data has a place with three distinct vintages 2000, 2001 and 2003 procured by Orient Petroleum Inc. in which 10 are plunge lines and four are strike lines. The orientation of lines and location of wells is shown in the base map (Figure1.2). The detail of these seismic lines is given in Table 1.1. All wells are gas condensate and drilled up to the Basal Sand (sands below Talhar shale) unit of Lower Goru. Information regarding well is given in the Table 1.2.

Table 1.1: Seismic data used for research work.

Seismic line	Nature	Seismic line	Nature
2000KH-04	Dip line	2001KH-24	Dip line
2000KH-06	Dip line	2001KH-30	Dip line
2000KH-08	Dip line	2003KH-35	Strike line
2001KH-11	Strike line	2003KH-36	Dip line
2001KH-13	Strike line	2003KH-39	Strike line
2001KH-20	Dip line	2003KH-40	Dip line
2001KH-22	Dip line	2003KH-44	Dip line

Table 1.2: Well log data.

Well name	Depth (m)	Formation Top (Basal Sand)(m)	Status of Wells	Discovery
Siraj South-01	3218.6900	3079.15	Exploratory	Gas Condensate
Bilal-01	3170.3501	3058.50	Exploratory	Gas Condensate
Naimat Basal-01	3599.6284	3479.10	Exploratory	Gas Condensate

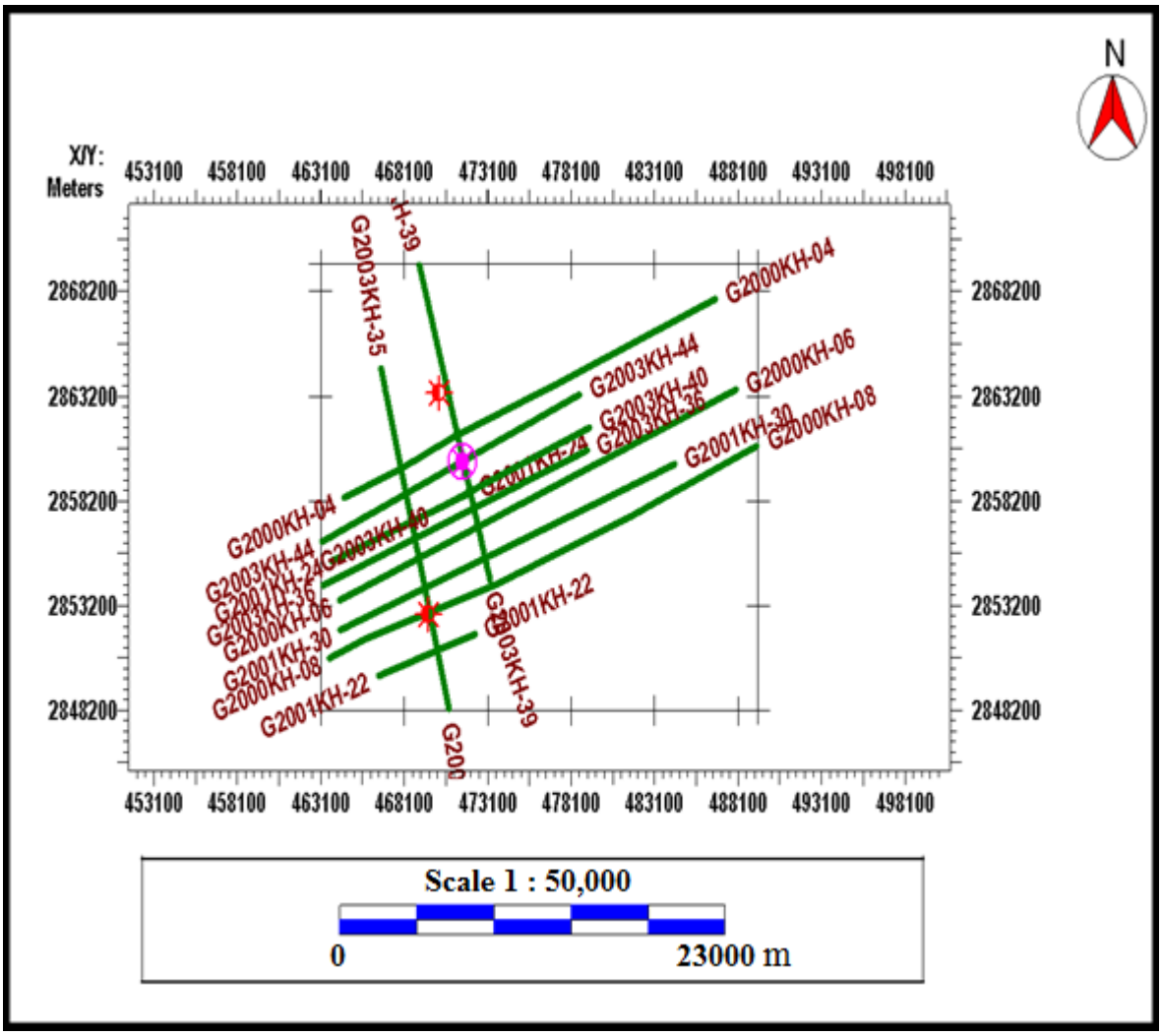

Figure 1.2 Base map of the area under study.

1.5 Motivation and Research Objectives

This research work is carried out with the aims to get the following research goals:

1 To make an understanding of the tectonics, structural settings and geology of the area to identify the petroleum play of study area.

2 To delineate the faults and horizons to understand the stratigraphic or structural traps by using 2D seismic interpretation.

3 To find out the zones which are hydrocarbon bearing by evaluating rock properties such as saturation of hydrocarbon and water, porosities etc. through petrophysical studies.

4 To develop a relationship between porosity and impedance to find out the porosity distribution all over the reservoir.

5 To predict pore pressure and to analyze normal compaction trend (NCT) using well log data.

6 To establish a relationship between inverted impedance and Pore Pressure using Probabilistic neural network approach.

1.6 Methodology

To achieve the above mentioned objectives methodology adopted is summarized and schematically illustrated in Figure 1.3.

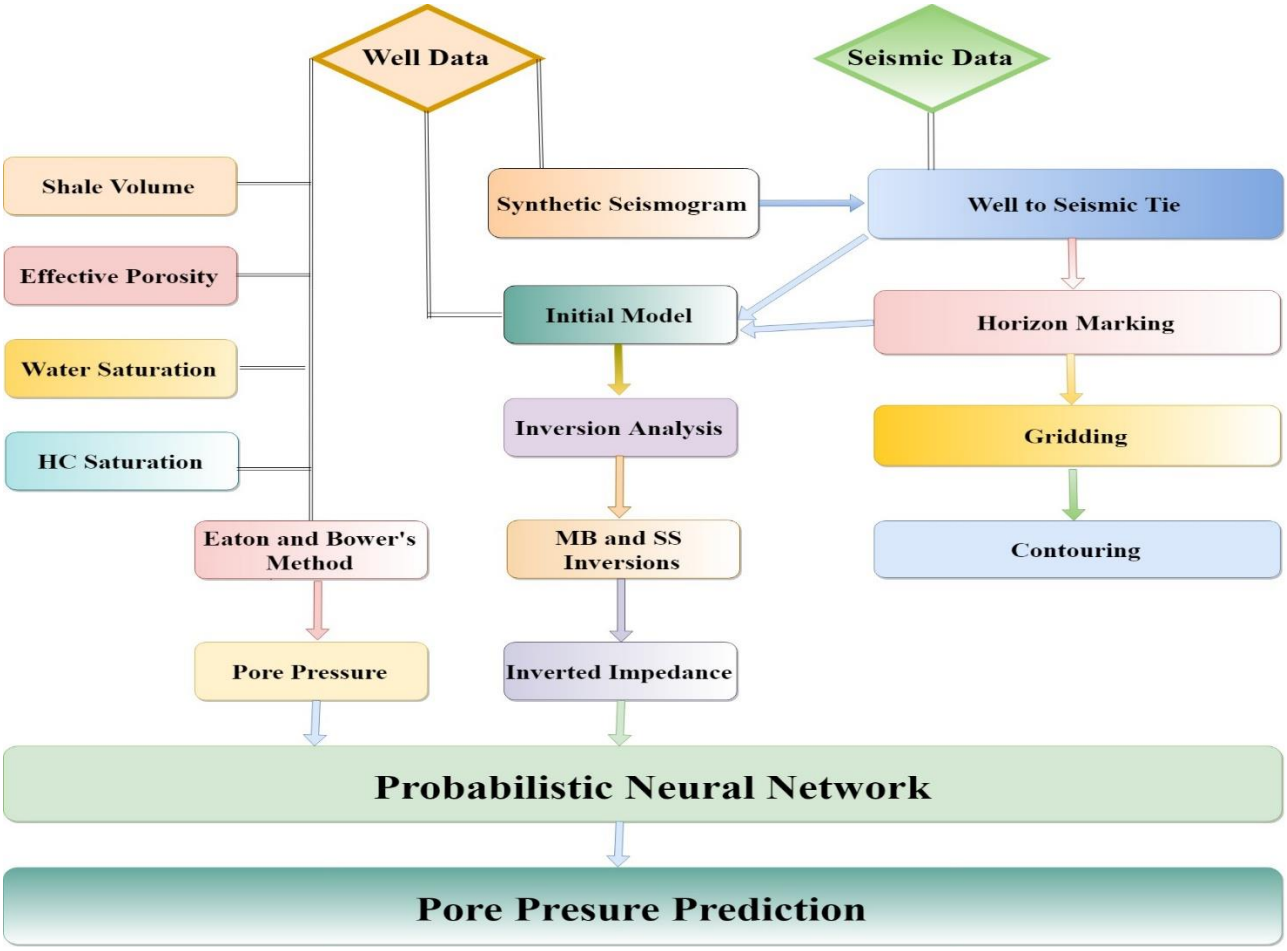

Figure 1.3 Methodology adopted for dissertation.

CHAPTER 2

GENERAL GEOLOGY

2.1 Sedimentary Basins

Basin is the area which can be defined by the subsidence of that region and in which the sediments are saved for the longer interval of time. The bowl which is fill or content, which is the assemblage of sediments settled on the basement, is called cover or sedimentary cover. Subsidence is the step wise fixation of the sediments in the basin. The mark of maximal sedimentary assemblage is termed as the Depocenter. The depocenter cannot be related to the area of maximum subsidence (Kazmi and Jan, 1997).

2.2 Basins of Pakistan

Pakistan is containing the following basins (Kadri, 1995);

1. Indus basin
    a. Upper part of the Indus basin
    b. Central part of the Indus basin
    c. Southern or Lower part of the Indus basin
2. Baluchistan basin
3. Kakar Khorasan basin

These basins are shown in Figure 2.1(b).

2.3 Structural Settings of Southern Indus Basin (Study Area)

Geological past of the Indus basin starts from the Precambrian age. This Indus Basin is defined mainly as Upper and Lower Indus Basin (central part of Indus Basin and southern part of Indus Basin). Sukhur rift (Jacobabad and Mari kandkot highs) mark the boundary between the central and southern part of Indus basin (Raza et al., 1990).

The area under study is situapted in southern side of Indus Basin which lies at southern side of the Sukhur rift. It contains the following important divisions.

- Thar Platform
- Karachi Trough
- Kirthar Foredeep
- Kirthar Fold Belt

The extension of trough and platform is into offshore Indus. Southern part of basin is extended up to Indian shield in the eastern side and up to the peripheral zone of Indian plate in the western side, its southern border is restrained by Murray ridge over fracture plate boundary (Kadri, 1995). The earliest rocks found here have its roots in Triassic age, southern and central part of Indus basin were not classified till lower or middle cretaceous, when khairpur Jacobabad high became a definite specific feature, marked by consistent lithologies found in Chilton limestone of Jurassic age and in Sembar formation of lower cretaceous age over the high. Goru formation's Sand facies from having age of lower or middle cretaceous are also continued up to kandkot and giandari area (Kadri, 1995).

Extensional tectonics result in generating normal faults, developing horst and Graben structures with former are important in terms of exploration. At the time of Cretaceous this extensional tectonics created the fault blocks which are tilted across vast area of Eastern flank of lower part of Indus basin (Khan et al., 1986). A passive roof complex breed structures and a passive back thrust are found in this lower part of Indus basin along Kirthar fold belt. This thrust forming a frontage culmination wall with the edge of the Kirthar depression, fold belt and out of syncline intra-molasses detachment in the Kirthar depression sequence (Zaigham and Mallick, 2000).

As the area of study Khipro is situated in the foreland side of the Himalayas, therefore normal faulting in the region is a common phenomenon. Generally faults are of low throw. Conjugate faulting often founds on small scale. Although book shelf geometry is present but as such no great structural changes found in Khipro

The style of structures in area is resultant of a normal block faulting on westward dipping Indus Plain. The fault planes provides a migrating paths to hydrocarbons underlying in source sequence which is shaly (Kadri, 1995). Directions of faults and horizons are summarized by exploiting seismic and wells control for the area of study. Basis for structural interpretation are created by interpreting the seismic as none of outcrops were found at the surface throughout the field. Study area is defined by a string of horst and graben structures found roughly beneath the base of Paleocene not beyond the Cretaceous age Producing reservoir, Basal Sand is surrounded

by regionally extended faults on both sides i.e. east and west which are dipping towards western and eastern side and leaning NW-SE (Kadri, 1995). Structural and Tectonic boundaries of the Khipro block are shown in the Figure 2.1.

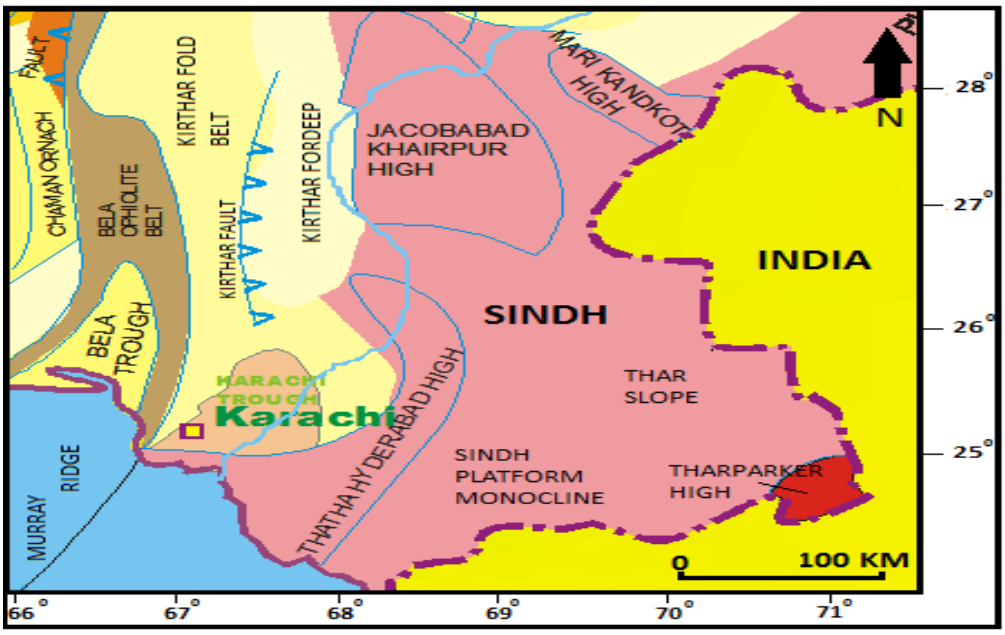

Figure 2.1 Basin architecture of the lower part of Indus Basin (Khan et al., 1986).

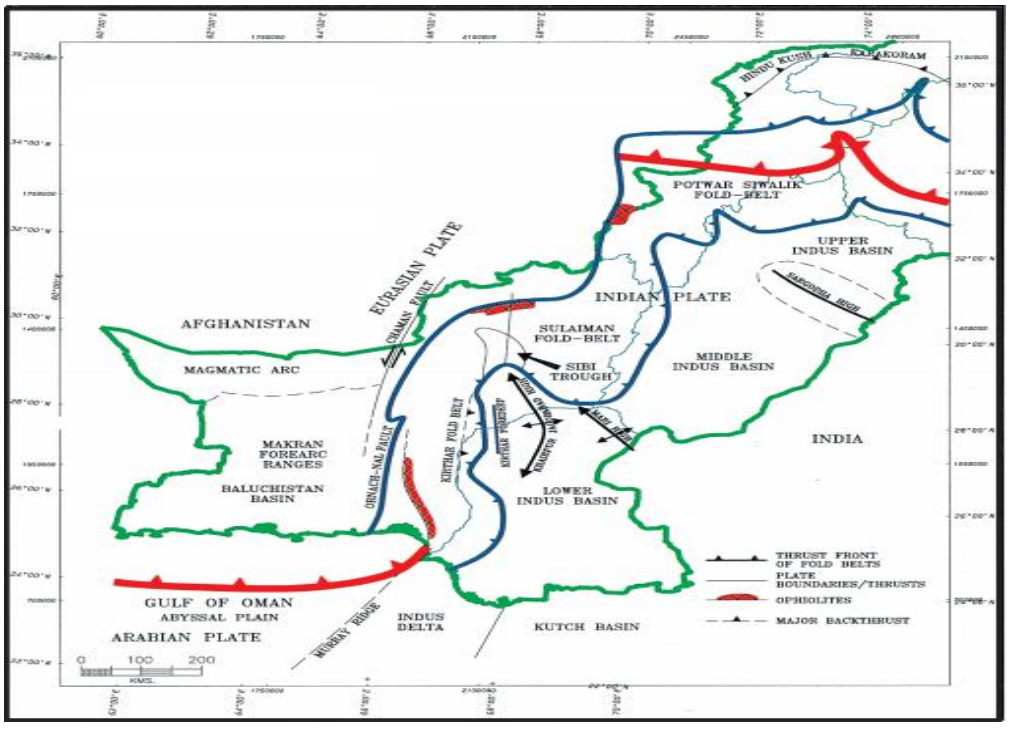

Figure 2.2 Tectonic scheme of Pakistan (Kazmi and Snee, 1989).

2.4 Regional Stratigraphy

Khipro area is situated in the southern sedimentary basin and geological studies has been carried out widely, summarized and its stratigraphy is vigorously defined. The structure has surface geological expressions.

The predicted stratigraphic sequences and lithologies were established on the basis of subsurface information and provincial stratigraphic knowledge. Almost all of the Pliocene to Infra-Cambrian sequences was well-known provincially (Shah, 1977).

A brief stratigraphic succession of lower part of Indus Basin is mentioned in the Figure 2.3 which illustrate that tectonic province under consideration is dominant by infra-Cambrian to lately carbonates and clastics. The array of stratigraphy alters when moved to west starting from east. Basement of Precambrian is found exposed at the southeastern edge of the basin. Sediments becomes thicker to westward. Crucial unconformity starts at the base of Tertiary. At eastern part, Tertiary succession has directly contacted with the Jurassic succession (Wasimuddin et al., 2004).

2.5 Stratigraphic Sequence of Khipro Area

The study area contains the rocks from early Cretaceous to recent with unconformities found between Cretaceous and Paleocene, and between Eocene and recent. The Stratigraphy of the study area is shown in table 2.1. Unconformities occur at base of Tertiary and at the base of recent rocks.

2.6 Petroleum Play of The Study Area

2.6.1 Source Rock

The Shale of Sember formation belonging to Lower Cretaceous age having enough organic content, thermally mature and containing oil prone kerogen type is justified source rock in the hydrocarbon discovered in this region. Richness of organic content in the deeper part of Lower Goru formation shale is medium having fair to good hydrocarbon bearing potential.

2.6.2 Reservoir Rock

The main zones of interest in this area is the Basal and Massive Sands (Sand below Talhar Shale) of Lower Goru Formation.

2.6.3 Cap Rocks

Massive succession of shale and marl from Upper Goru as well as shale contained by Lower Goru act as cap rock for the sandstone reservoirs those are underlying them.

Table 2.1. Stratigraphy of the study area.

Age	Formation	Lithology
Recent	Alluvium	Sandstone containing subordinate clay or claystone and conglomerate rarely found.
Eocene	Kirthar	Limestone.
Paleocene	Ranikot	Sandstone is interbedded along with shale and fine beds of Limestone and clay or claystone.
	Khadroo	Volcanics, Basalts.
Cretaceous	Parh	Limestone and chalk.
	Upper Goru	Marl with minor shale and limestone.
	Top Lower Goru	Shale with subordinate sandstone, marl, siltstone and rare limestone.
	Upper Shale	Shale.
	Middle Sand	Sandstone with Siltstone and Marl.
	Lower Shale	Shale.
	Sand Above Talhar Shale	Sandstone with subordinate shale.
	Talhar Shale	Shale with minor traces of sandstone and siltstone.
	Sand Below Talhar Shale	Sandstone with subordinate shale.

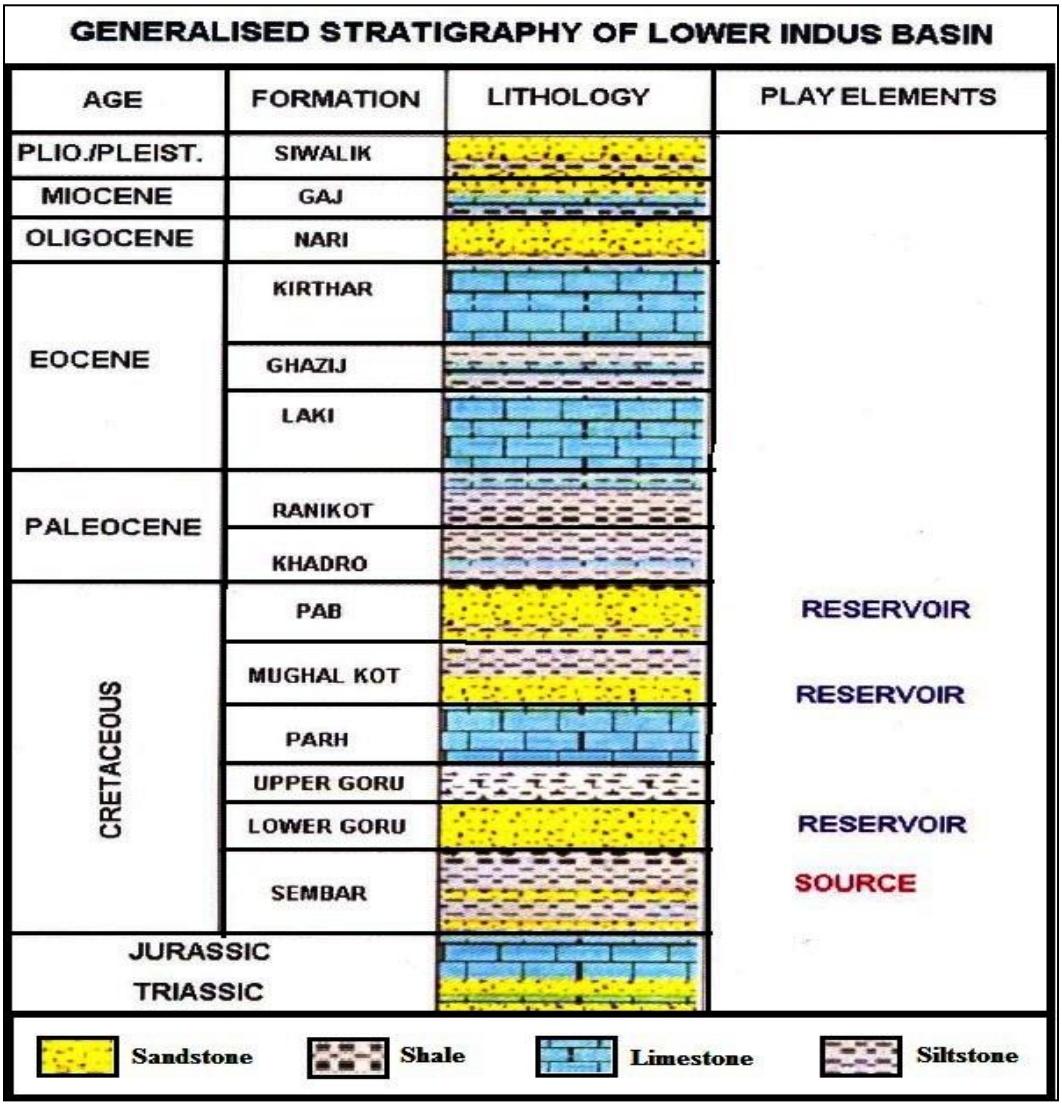

Figure 2.3 Stratigraphic Succession of lower part of Indus Basin (Khan et al., 1986).

CHAPTER 3

SEISMIC DATA INTERPRETATION

3.1 Introduction

Interpretation of seismic data is the conversion of seismic data to structural and stratigraphic image by applying the course of distinct steps.

Seismic reflections occurs along boundaries across which there is a contrast in acoustic impedance. Velocity and density product gives us the acoustic impedance. The greater the contrast, the stronger will be the reflection.

Seismic reflection meaning is a sign of an acoustic barrier which needs to be recognize that in case this boundary spot a fault or a stratigraphic connection with any other boundary. Those features needs to be pointed which are not pointed by the sharp boundaries (Badley, 1985). There are two main approaches which are generally used to interpret the seismic sections:

a. Structural interpretation

b. Stratigraphic interpretation

3.2 Structural Interpretation

The aim of structural interpretation is to search for the structural traps that contain hydrocarbons. Generally, the structural interpretation is carried out by generating time and depth contour maps. The most common structural features associated with the hydrocarbons are anticlines and faults. This research work deals with the structural interpretation.

3.3 Stratigraphic Interpretation

Seismic Stratigraphy often used to spot out the deposition means and environmental framework. These traps may be originated from the features associated with erosional truncation e.g. pinch outs and reefs etc.

3.4 Workflow for Interpreting Seismic Data

Procedure followed for seismic data interpretation is given in Figure 3.1. Base map is set up by means of navigation and SEG-Y files in SMT kingdom. Horizons of concern are pointed manually, also through auto-tracking. At first horizons are identify by means of synthetic seismogram, which is generated using well data. In this method faults are recognized and also pointed out. Fault polygons created and horizons were contoured to catch on structural lows or

highs. Contour maps of time and depth were computed. Depth contours were computed by means of well point velocity.

Figure 3.1 Workflow for seismic data interpretation.

3.5 Identification of Seismic Horizons

Basic and key job for understanding of seismic data is actually the demarcation of several horizons as a boundary among geological formations. For this, accurate information regarding structure as well as stratigraphy of area is mandatory. Therefore to fulfil the earliest step of the interpretation, two horizons were picked with the aid of synthetic seismogram of the Naimat Basal-01. It is drilled at shot points 357 and 290 of lines 2000KH-08 and line 2003KH-35. Two horizons

are picked on line 2000KH-39 and 2000KH-08 while remaining line horizons were picked using digitize arbitrary line technique. Picked horizons are Lower Goru and Basal Sand.

3.6 Generation of Synthetic Seismogram

For generation of synthetic seismogram two way time for each well top is required. Two way time for reflector is calculated using depth, sonic data of well and replacement velocity of the area. Using two way time against each depth, time depth chart is prepared. Then finally synthetic seismogram is generated by convolving the well data and extracted wavelet having frequency of 50Hz. Tied this synthetic seismogram with the Seismic line, on which well is located 200KH-08 and 2003KH-39. Synthetic seismogram of Naimat Basal-01 is shown in Figure 3.2.

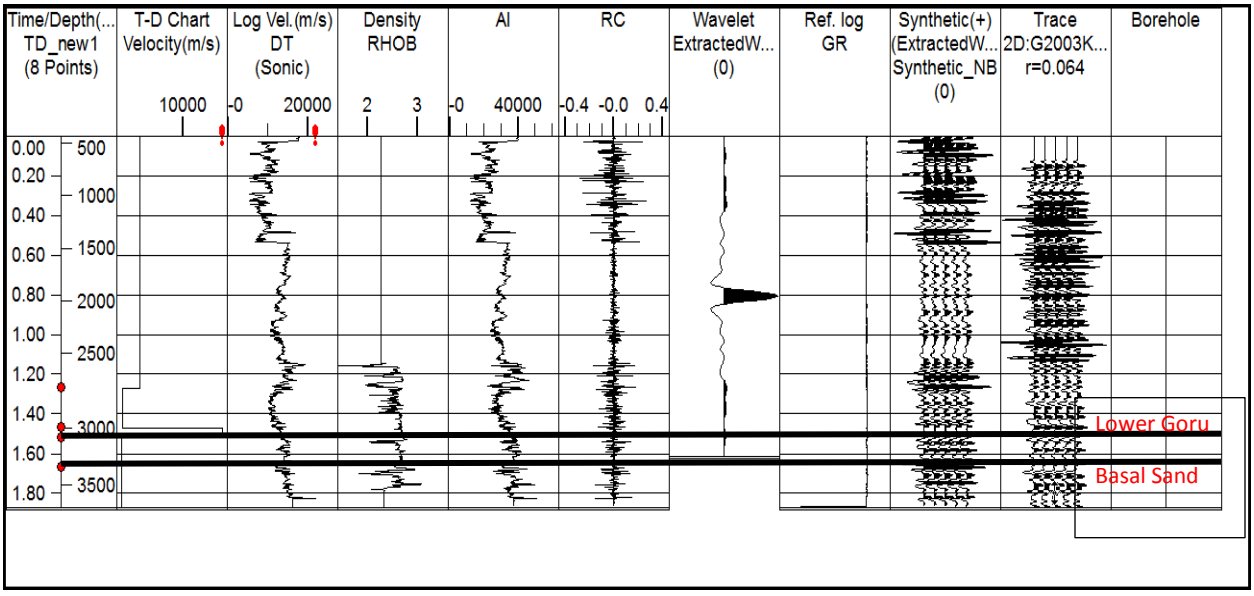

Figure 3.2 Synthetic seismogram of Naimat basal-01.

3.7 Marked Seismic Sections

Two seismic horizons Basal Sand and Lower Goru (of early cretaceous age) are marked. Along these seismic horizons, eight faults are also picked. Interpreted seismic sections of the assigned lines are shown in Figure 3.3, 3.4, 3.5, and 3.6. These seismic section shows Horsts and Grabben structure except line 2000KH-35 which is a strike line. Structures are not clear in strike line therefore faults are not marked. These Horsts and Grabben structures are related with normal faulting that illustrates study area situated in extensional regime.

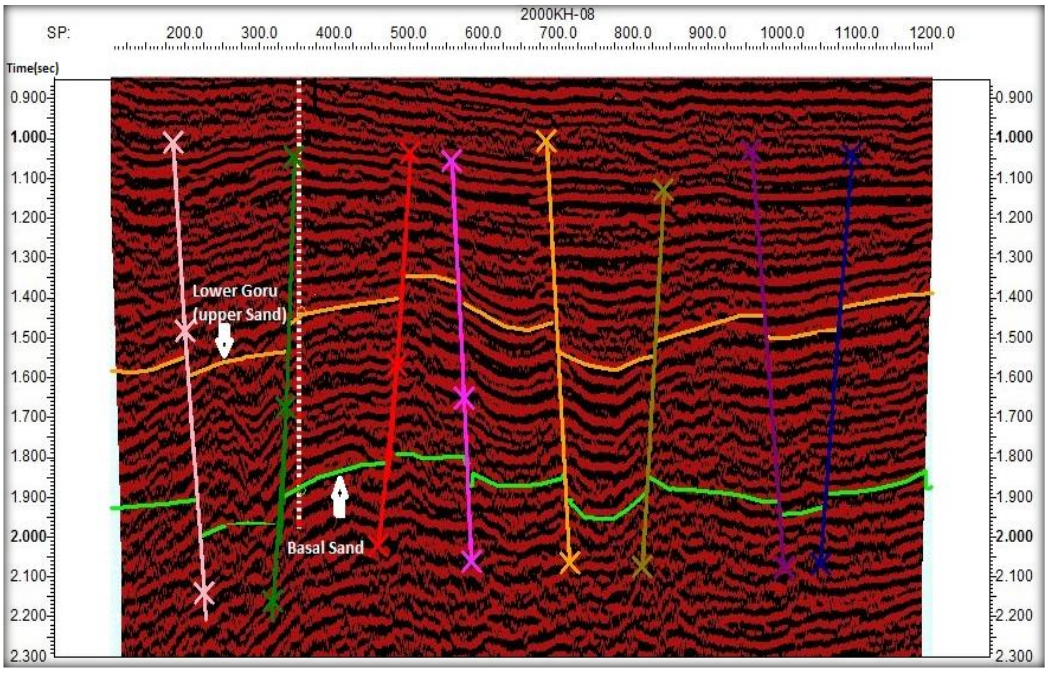

Figure 3.3 Interpreted time section for line 2000KH-08.

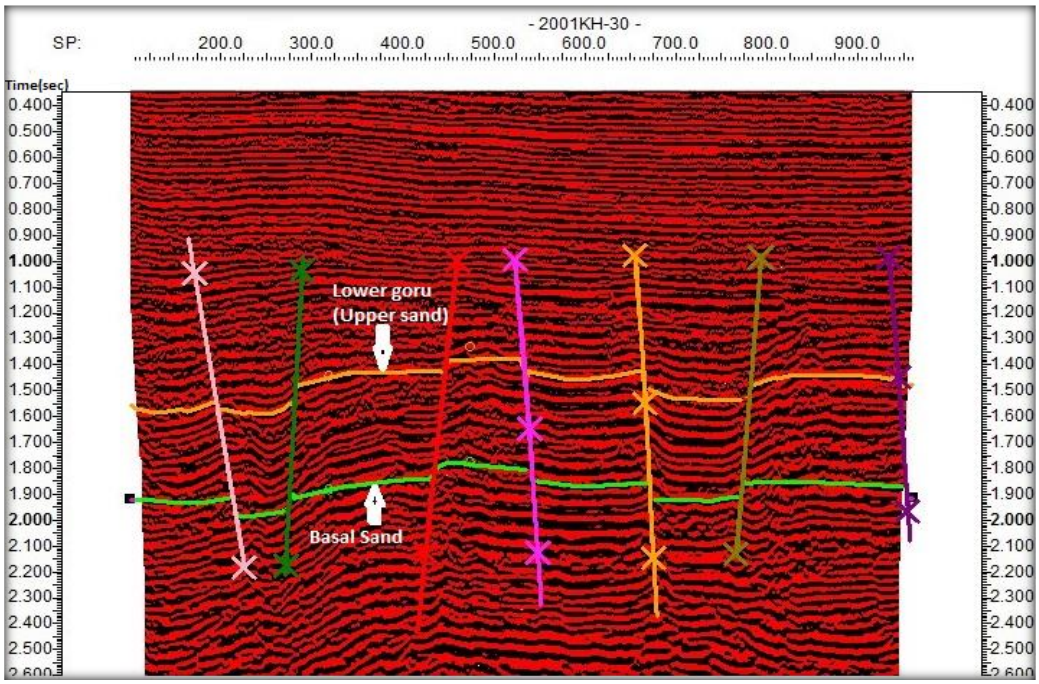

Figure 3.4 Interpreted time section for line 2000KH-30.

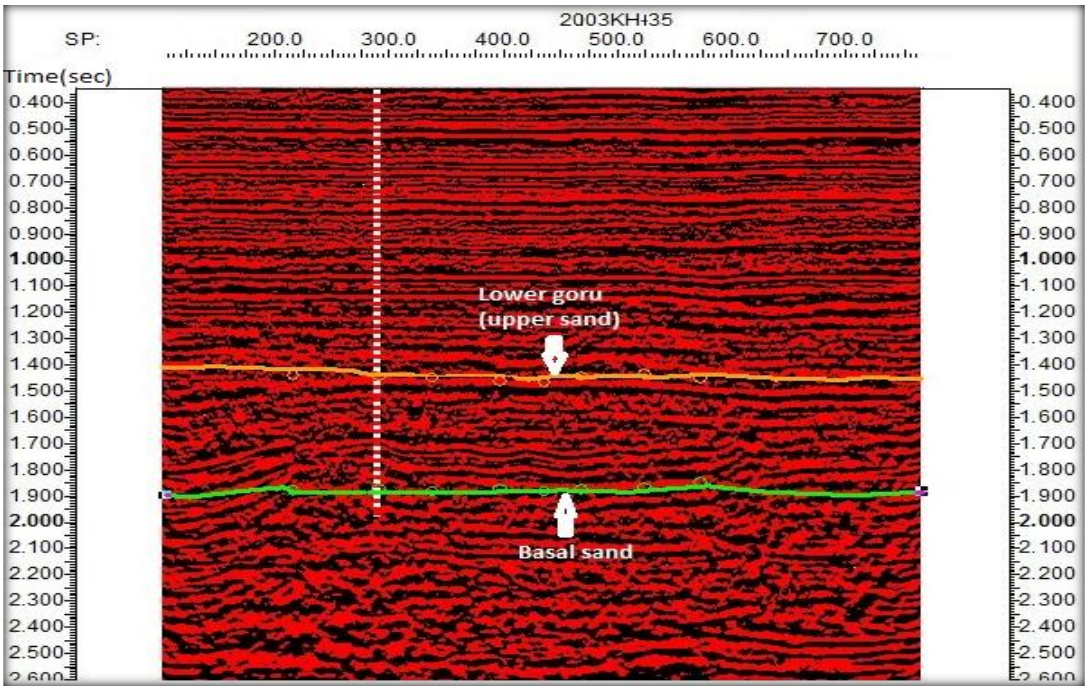

Figure 3.5 Marked seismic section for line2003KH-35.

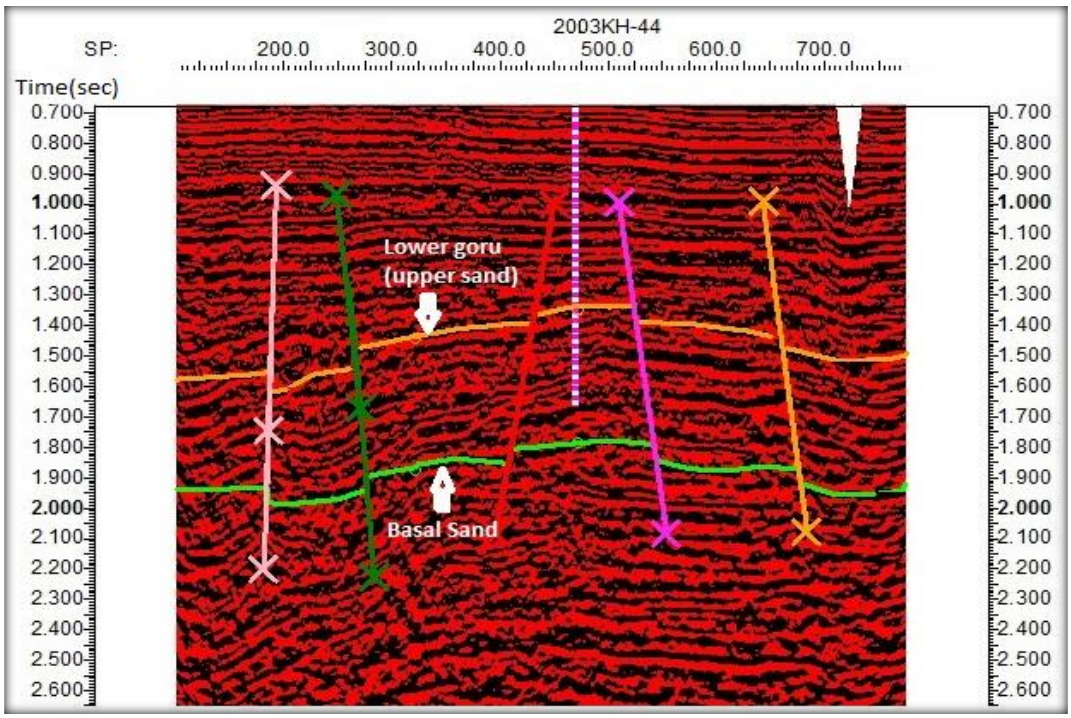

Figure 3.6 Marked seismic section for line2003KH-44.

3.8 Constructing Fault Polygon

Constructing fault polygons is highly significant as much as contouring of a specific horizon in time or depth is concerned. All mapping software demands that all faults should be changed in to polygons before contouring. Purpose is that, if any fault is not converted into a polygon, then software doesn't spot it as a breaks, therefore creating any probable closures against faults leads to a false portrait of subsurface. Figure 3.7 and 3.8 are made at Lower Goru and sand above Talhar shale level displays that afterward construction of fault polygons, low and high regions on a specific horizon become clear. Furthermore, the related color bar supports regarding dip directions. Construction of fault polygons is done for all picked horizons and they were oriented in NE-SE.

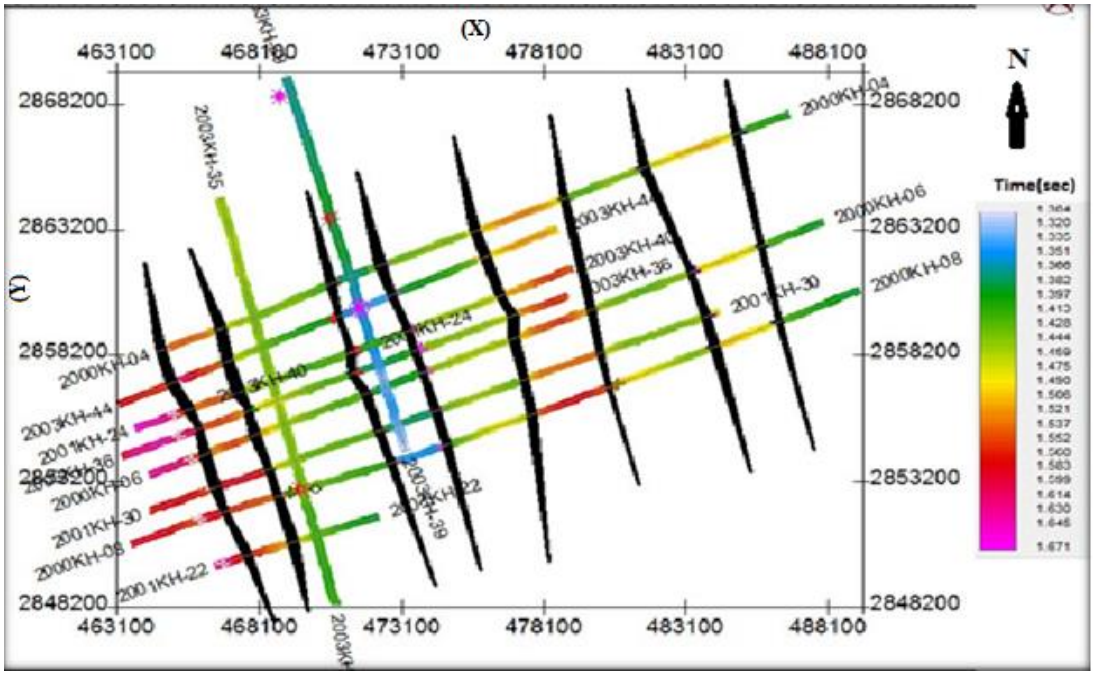

Figure 3.7 Fault polygon at Lower Goru horizon.

3.9 Contour Maps

Main tool utilized in the seismic interpretation is contouring. What sort of structure is forming a particular horizon becomes obvious after contouring. Formation is selected for the sake of computing contour maps. In making a subsurface map from seismic data, a reference datum must be selected. The datum might be sea level or any other depth above or below sea level. Normally, additional datum above sea level is selected so as to image a shallow marker on the

seismic cross-section, which might have a great effect on the interpretation of the zone of concern (Gadallah and Fisher, 2009).

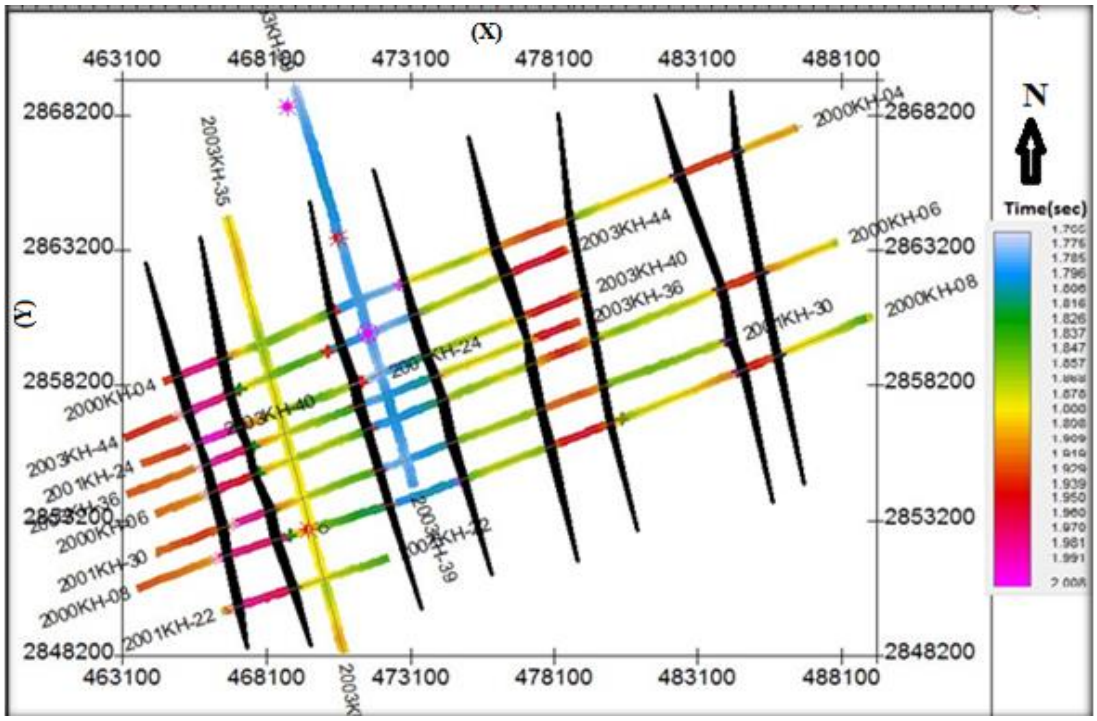

Figure 3.8 Fault polygon at Basal sand horizon.

3.9.1 Time Contour Maps

Time contours shows horizontal as well as vertical variations in time at the level of horizons. Time contour maps are computed at Lower Goru and sand above Talhar shale level, Figure 3.7 and 3.8 respectively. Color deviations clearly presenting the horsts and grabben structure. Brighter color indicates comparatively shallower part while darker color indicates comparatively deeper part. Trend of both maps is similar which indicates there is no vertical variation. Both horizons distort equally by faulting.

3.9.2 Depth Contour Maps

Depth contour are computed by means of well point velocity. Depth contour maps also indicates horizontal variation with respect to depth. The trend of depth contour maps is identical as of time contour maps because there is same horizontal variations with time as well as depth. Depth contour maps at Lower Goru and sand above Talhar shale level are shown in Figure 3.9 and 3.10 respectively. From the Figures, it is clear that Horsts and Grabben structures are formed those also formed in time contour maps.

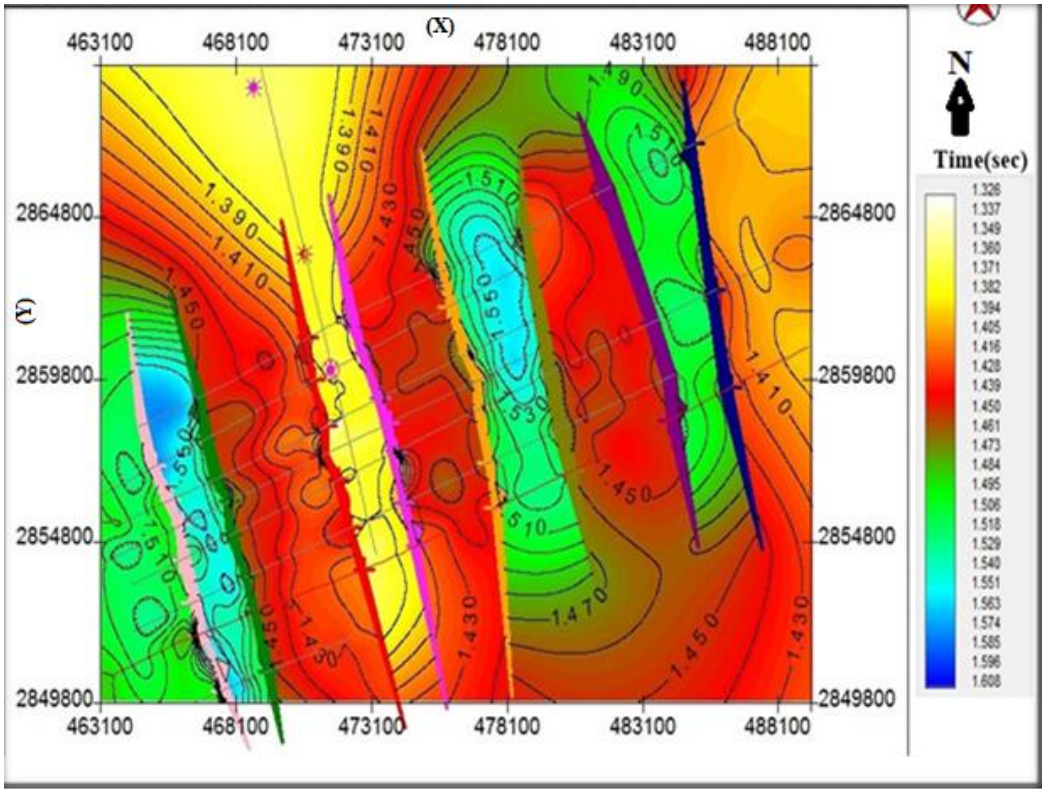

Figure 3.9 Time contour map at Lower Goru horizon.

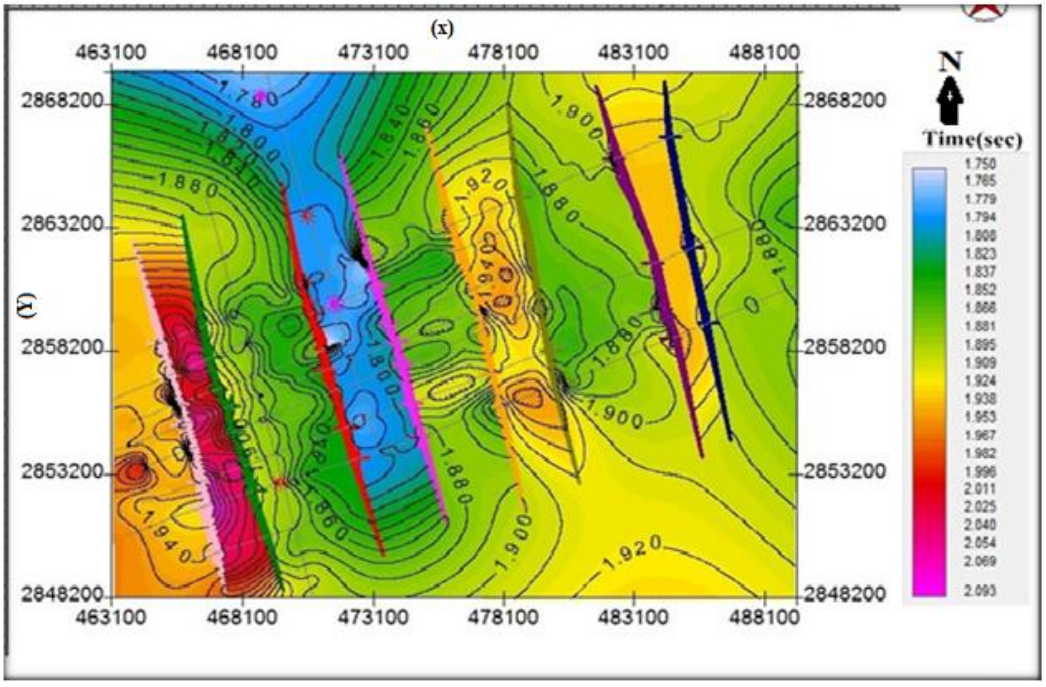

Figure 3.10 Time contour map at Basal sand horizon.

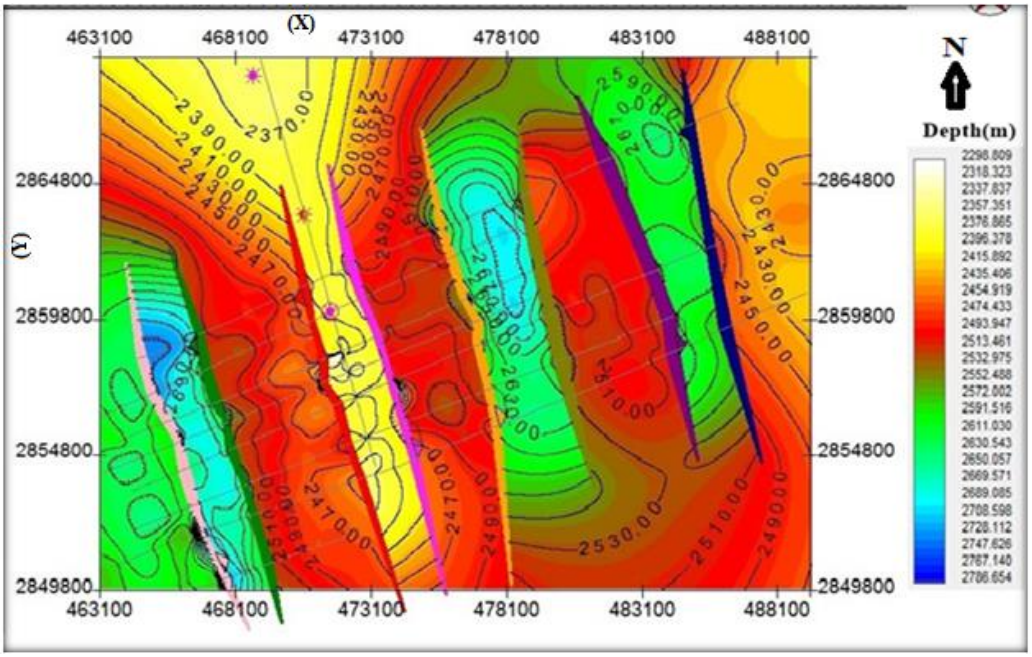

Figure 3.11 Depth contour map at Lower Goru horizon.

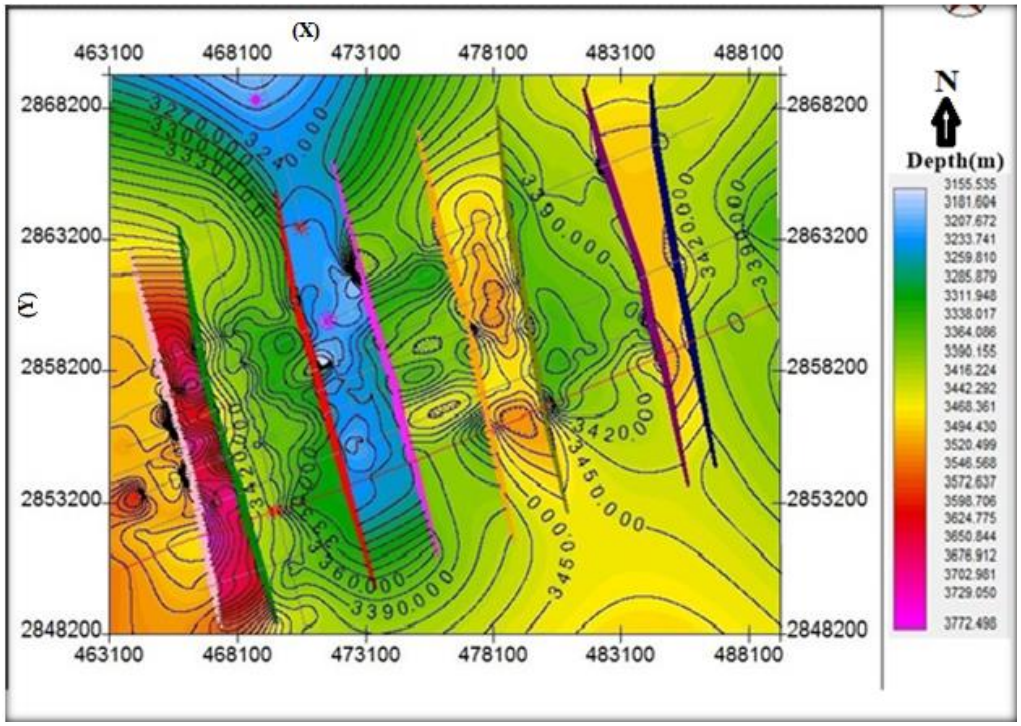

Figure 3.12 Depth contour map at Basal Sand horizon.

CHAPTER 4

WELL LOG ANALYSIS

4.1 Introduction

Petrophysics is the review of physical characteristics that define the existence and nature of fluids, rocks and soils. Normally a chain of task is performed in order to reveal the hydrocarbon potential of the formation. To find out the hydrocarbon saturation in the reservoir different parameters are calculated (Petro-consultant, 1996). The entire workflow for well log analysis is mentioned in Figure 4.1.

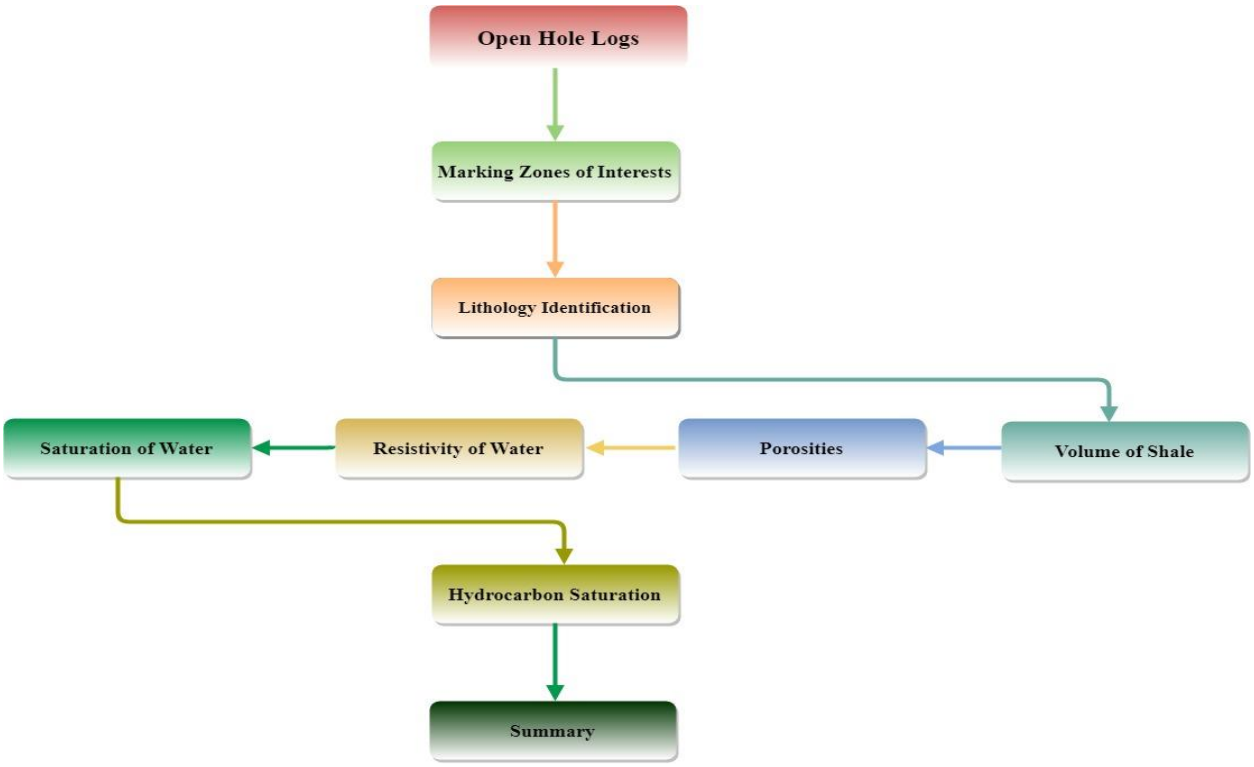

Figure 4.1 Workflow followed for the petrophysical analysis.

The earlier stage while analysing well log, is to point out the section of concern in raw log. Some of key petrophysical properties e.g. shale volume (Vsh), voids (φ), water resistivity (Rw), Water Saturation (Sw) are calculated from the logs. Present studies covers sands of Naimat Basal-

01 and Siraj South-01 well. Log data are available from 3495 to 3545m in Naimat Basal-01 and from 3080 to 3140 m in Siraj South-01.

4.2 Scheme for Log Analysis

4.2.1 Quantifying Clay

Volume of clay can be determined with the aid of gamma ray log and the clean and shale values are selected in the gamma ray.

4.2.2 Quantifying Shale

Particularly Gamma ray helpful for delineating shale beds. Gamma ray depicts the amount of shale and it can be helpful for indication of shale and also a terrific bed marker. Gamma ray furthermore differentiate the shaly zone from clean one. (Petro-consultant, 1996). While quantifying the shale content, volume of shale was computed with the aid of following expression mentioned below:

$$V_{sh} = \frac{GR_{\log} - GR_{min}}{GR_{\max} - GR_{min}}$$

where:

V_{sh} is amount of shale

GR_{log} is value of GR at specific point

GR_{min} is minimum value of GR across interval

GR_{max} is maximum value of GR across interval

4.2.3 Porosity Computation

Ratio of pore spaces to the entire volume of rock is the Porosity. It is expressed in percentage or as a decimal fraction and is represented by ϕ (phi). The combination of neutron and density is used commonly to compute porosity. Acoustic log is furthermore helpful for porosity computation and is a measure of the transit time versus depth of higher frequency acoustic pulses through formations close to the borehole.

Bulk density of formation (φ_{den}) is dependent of density of matrix, fluid density in the voids (hydrocarbons, salty or fresh mud) and porosity. The expression to compute porosity from density is (Cannon, 2016):

$$\emptyset_{den} = \frac{\rho_{-ma} - \rho_{\_b}}{\rho_{\_ma} - \rho_{\_f}}$$

Here:

φden = Density derived porosity

ρ_ma = Matrix density

ρ_b = Formation bulk density

ρ_f = Fluid density

Average porosity is computed using the following equation:

$$\emptyset_{avg} = \frac{D_{phi} + N_{phi}}{2}$$

Where:

$\emptyset_{avg}$ is the Average porosity.

D_{phi} is the density porosity.

N_{phi} is the neutron porosity.

Effective porosity is combination of all the pore spaces that are interconnected and relate to total porosity. Effective porosity can be computed by applying the following equations (Cannon, 2016):

$$\emptyset_{eff} = \emptyset_{avg} * (1 - V_{shl})$$

Where:

$\emptyset_{eff}$ is effective porosity

$\emptyset_{avg}$ is mean porosity

V_{shl} is amount of shale

V_{sand} is amount of sand $(1 - V_{shl})$

4.2.4 Water Resistivity (Rw)

Water resistivity can be computed using two methods, one by applying schlumberger chart, alternative method is by mathematically from S.S.P. To determine R_w the Static Spontaneous Potential (S.S.P) was computed against a clean porous bed, where maximum deviation in the SP log. Then temperature of formation is computed. After this, resistivity of mud filtrate (Rmf), is calculated.

Schlumberger SP-2 graph is applied to derive the value of R_{mfeq} at temperature of formation. The maximal deviation on SP curve is pointed out and R_{weq} is computed with the aid

of Schlumberger SP-1 graph by pointed out $R_{mfeq.}/R_{weq.}$at temperature of formation. Using this computed value, R_{mfeq} value pass to compute R_{weq}. Finally, SP-2 graph is applied to put R_{weq} and compute R_w against the temperature of formation.

4.2.5 Saturation of water

Saturation of water (Sw) can be computed with the aid of Archie Equation (Gibson, 1982)

$$(Sw)^n = \frac{a}{\phi^m} * \frac{Rw}{Rt}$$

Here:

S_W is Saturation of Water

n is Exponent of Saturation

a is Coefficient of Lithological

Φ is Effective Porosity

m is Factor for Cementation

R_w is Water Resistivity

R_t is True/ Deep Resistivity at that depth.

The a, m, and n values are considered to be constant.

$N = 2$

$m = 2$

$a = 1.63$

By inserting values of mentioned parameters and reducing the above equation it looks like:

$$Sw\ (\%) = \sqrt{\frac{1}{\phi^2} * \frac{Rw}{Rt}} * 100$$, (Gibson, 1982)

4.2.6 Hydrocarbon Saturation

Hydrocarbon saturation is computed with the aid of formula given below. The value is multiplied with 100 to represent in percentage.

$$S_h = (1 - SW) * 100$$

4.3 Petrophysical Analysis of Naimat Basal-01 and Siraj South-01

Well logs of Naimat Basal 01 and Siraj South 01 are shown in Figure 4.2 and 4.3 respectively. Caliper log gives borehole diameter information. Gamma ray helps in lithology identification; i.e. shale or sand. Shale has higher gamma ray values as radioactive minerals are

present in shale. Lower gamma ray values indicate sands. Laterologs measure resistivity. Separation in Laterologs (LLS and LLD) indicate pore spaces.

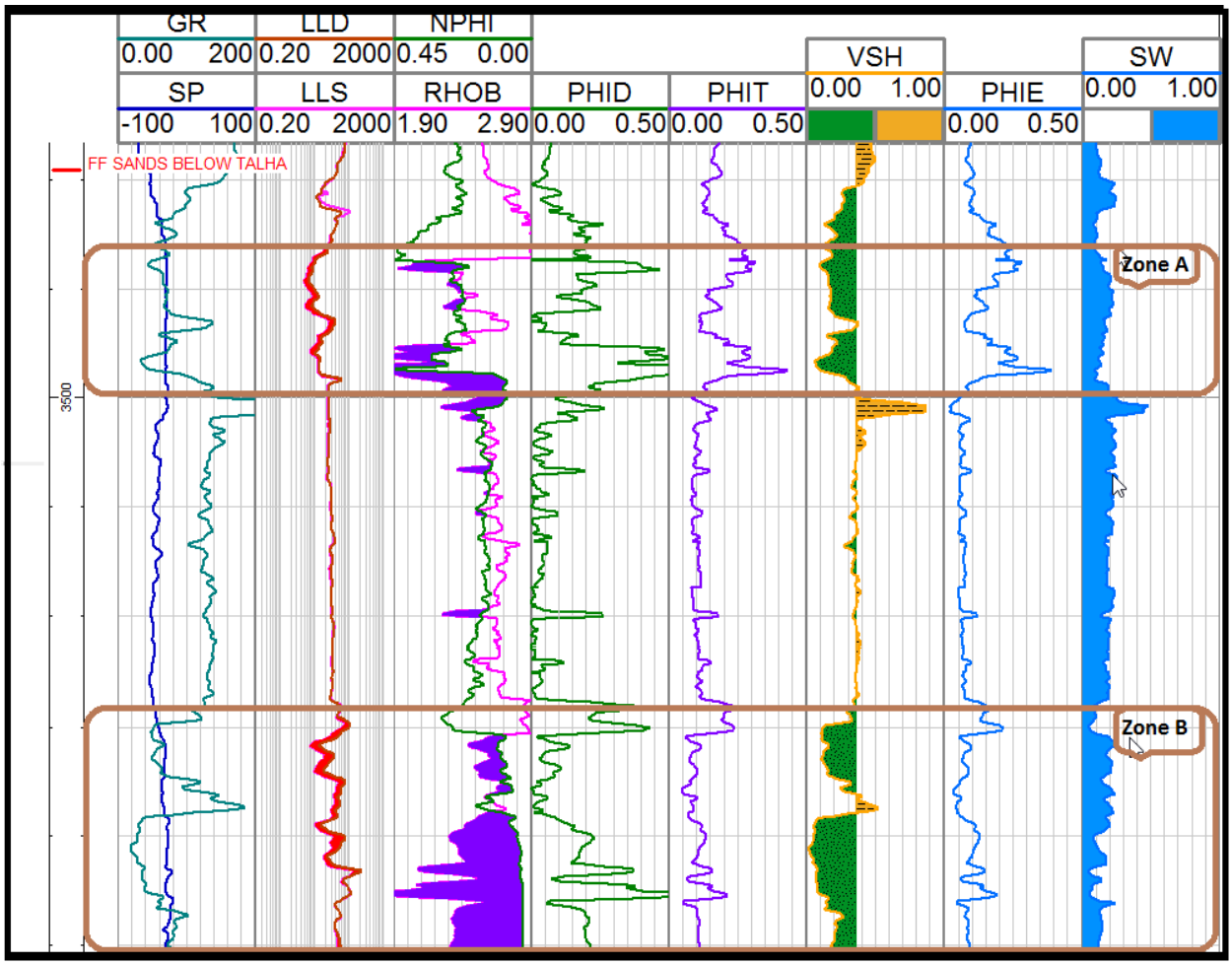

Figure 4.2 Well Logs of Naimat Basal 01.

The well logs of Naimat-Basal-01 are shown at target of interest i.e. Sand below Talhar Shale. Two prominent zones are marked as Zone A and Zone B as a reservoir zones.

Zone A: High values of SP log at 3485 to 3500 m shows caving in the bore hole at this depth, Gamma ray is decreasing indicating sands. Separation between Laterologs and presence of crossover between RHOB and NPHI indicates the presence of hydrocarbons. High resistivity values with separation between Laterologs and RHOB, NPHI crossover indicates gas. Medium resistivity values with separation between Laterologs and crossover between RHOB and NPHI indicates Oil. This is because resistivity of gas is higher than resistivity of oil.

R gas > **R** oil> **R** water

In this zone resistivity has medium values with separation and good crossover between RHOB and NPHI is observed thus indicating oil. This zone have very good effective porosity of almost 20% and very low water saturation of about 18%.

Zone B: This zone starts from 3528m to 3150m. Lower values of gamma ray, separation of resistivity logs and a good crossover between Density and Neutron logs indicate that this zone might have good quantity of hydrocarbons in it. Good values of effective porosities and lower values of water saturation further strengthen the previously mentioned indication.

The well logs of Siraj South 01 are show at target of interest i.e. Sand below Talhar Shale. Different zones are marked as Zone A, B and C as a reservoir zones.

Zone A: From 3066 to 3074 gamma ray is comparatively on lower side indicating sands, separation between LLD and LLS and crossover between RHOB and NPHI can be clearly seen in Figure 4.3. Effective porosity is about 12% and SW below 20% confirms the reservoir zone

Zone B: From 3115 to 3127m gamma ray is again comparatively on lower side which is indication of presence of sands, separation between Laterologs and a good crossover between RHOB and NPHI clearly marked and can be seen in Figure 4.3. Effective porosity is about 20% and SW is low and below 20% confirms the good reservoir zone

Zone C: From 3164 to 3172 m again some sands reappears and separation between Laterologs can be seen with a very good crossover of RHOB and NPHI indicating presence of hydrocarbons. Less shale, more sand, slightly more effective porosity is present at this depth.

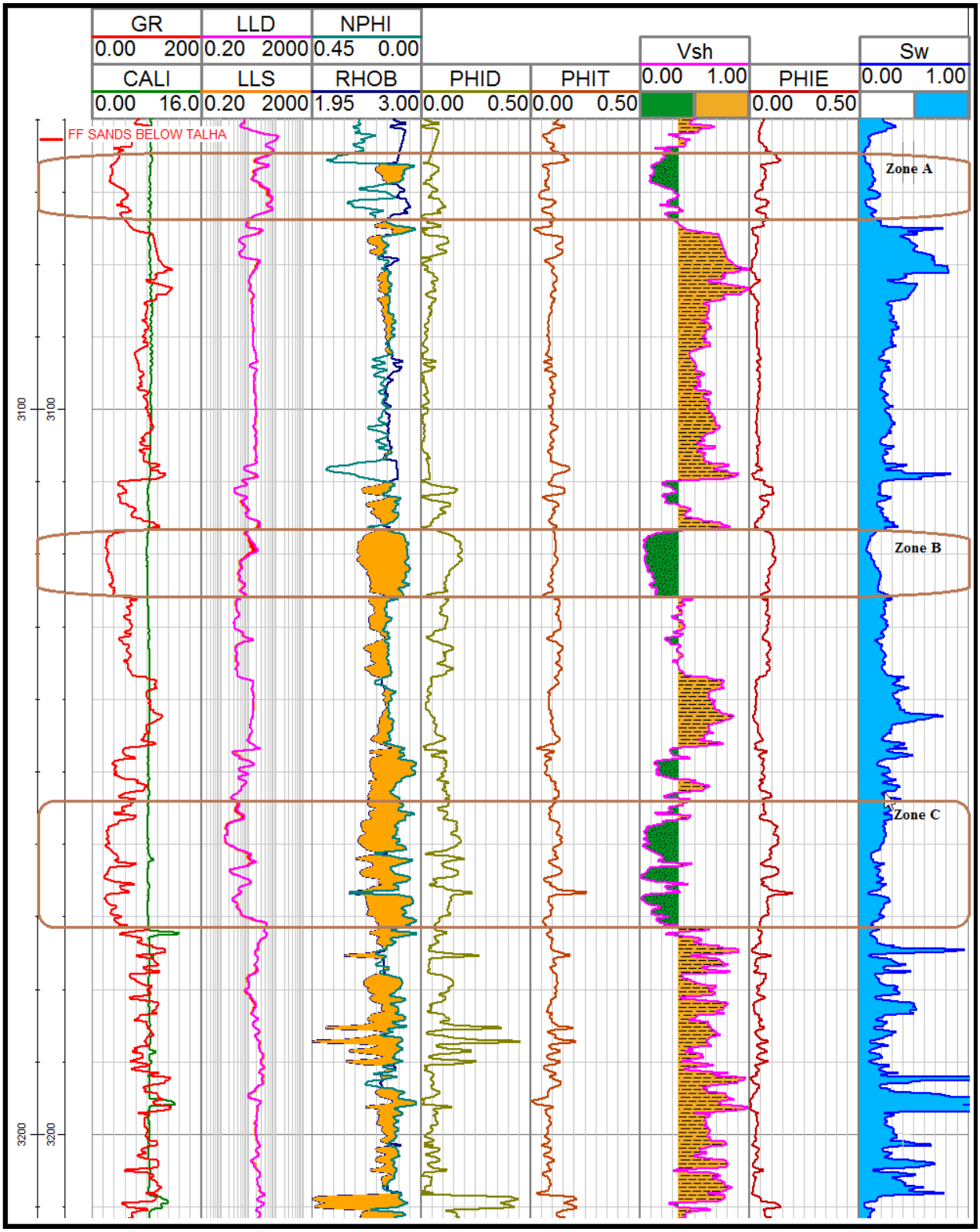

Figure 4.3 Well Logs of Siraj South 01.

Table 4.1: Calculated Petrophysical Parameters for Naimat Basal-01.

Calculated Petrophysical Parameters	ZoneA	ZoneB
Depth	**3485m to 3500 m**	**3530m to 3550m**
Average Volume of Shale	**19.4 %**	**15.7%**
Average Total Porosity	**20.8 %**	**10.5%**
Average effective Porosity	**17.2 %**	**9.0 %**
Average Water Saturtion	**15.6 %**	**14.8 %**
Average H.C Saturtion	**84.4 %**	**85.2 %**

Table 4.2: Calculated Petrophysical Parameters for Siraj-South-01.

Calculated Petrophysical Parameters	ZoneA	ZoneB	ZoneC
Depth	**3063 to 3070m**	3116 to 3127m	3155 to 3172m
Average Volume of Shale	**19.6 %**	16.6 %	17.14 %
Average Total Porosity	**9.3 %**	10.7 %	10.7 %
Average effective Porosity	**7.4%**	8.84 %	8.9 %
Average Water Saturtion	**9.5 %**	16.5 %	19.6 %
Average H.C Saturtion	**90.5 %**	83.5 %	80.4 %

CHAPTER 5

POST STACK SEISMIC INVERSION

5.1 Introduction to Seismic Inversion

For the identification of hydrocarbon potential reservoirs, one of the best techniques in seismic exploration is 3D seismic surveying. However traditionally 2D method is mostly in practice which is used to determine the depth and geometry of the target horizons. Whenever seismic wave intercepted at interface because of acoustic impedance contrast, these potential properties of the layer can be determined (Veeken and Silva, 2004).

Geophysical inversion is a technique in which physical properties of subsurface may be computed using observed geophysical data. It may called as seismic inversion if it applied on seismic data. Input data used for computing earth's physical characteristics are usually sonic, density logs, seismic data and streak of interpreted horizons are common data collections that are utilized as input data for post stack seismic inversion (Figure 5.1). Post stack seismic inversion is defined as, if this is applied after stacking of seismic data and pre stack seismic inversion is defined as if it is applied on pre stack data with multi offset suppositions.

Process of inversion includes comparison, computation and other methodologies such as guessing in order to make an inference by utilizing the real data recorded in the field. Hence inversion is a set of mathematical procedure that is used to reduce real field data with aim of extracting valuable information such as physical properties of the reservoir based on the inference which was drawn on observed values (Sen and Stoffa, 1995). Estimating reservoir properties such as porosity is major goal of seismic inversion. Seismic inversion is extremely useful while monitoring variations in properties of rocks due to oil or gas production, fluid injection, reservoir characterization or planning a well at some suitable location (Gavotti et al., 2014).

In Post stack type of inversion have zero offset suppositions practiced commonly on refined stacked data, commonly referred as acoustic impedance inversion otherwise seismic inversion, characteristics of reservoir all across may be anticipated from an impedance volume resulted, aside from well domain (Figure 5.2).

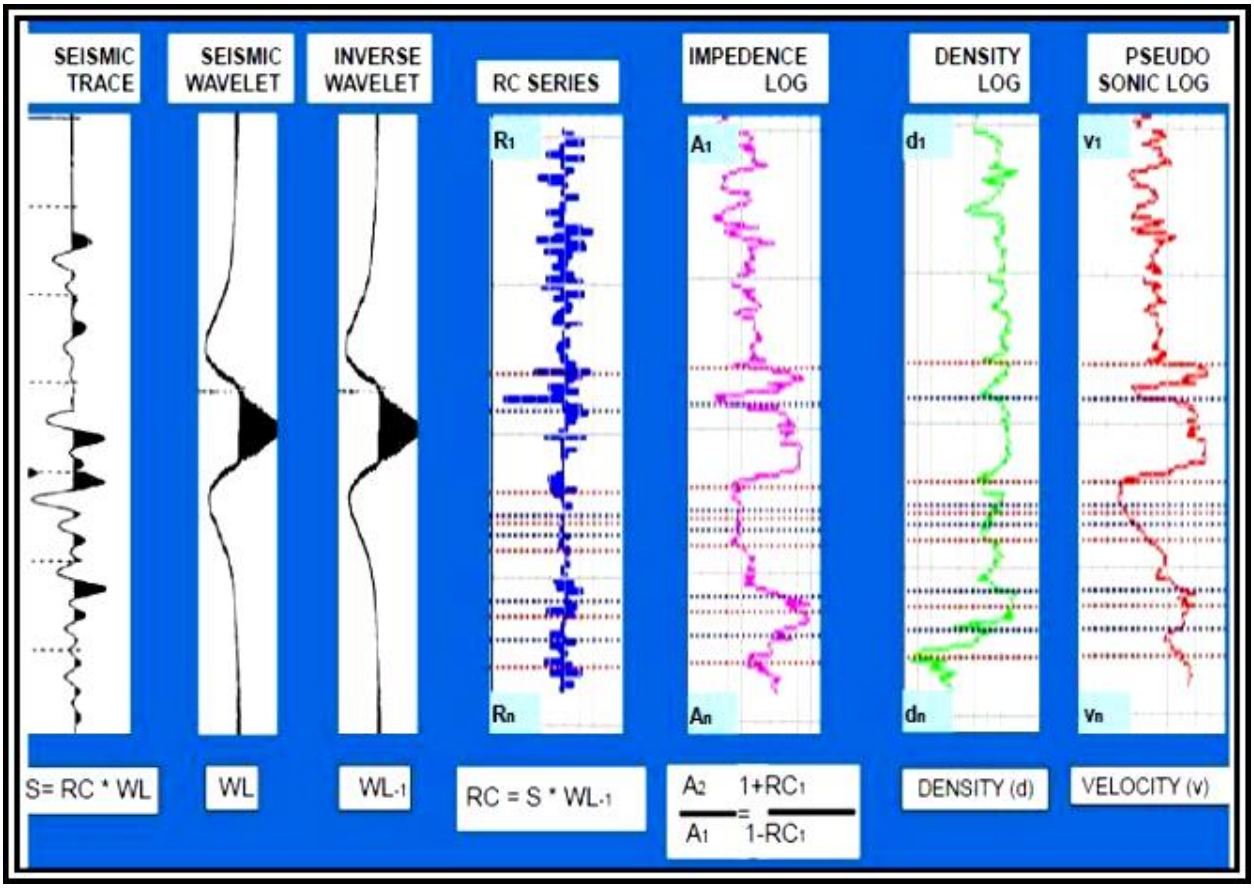

Figure 5.1 Work flow of seismic inversion (Veeken and Silva, 2004).

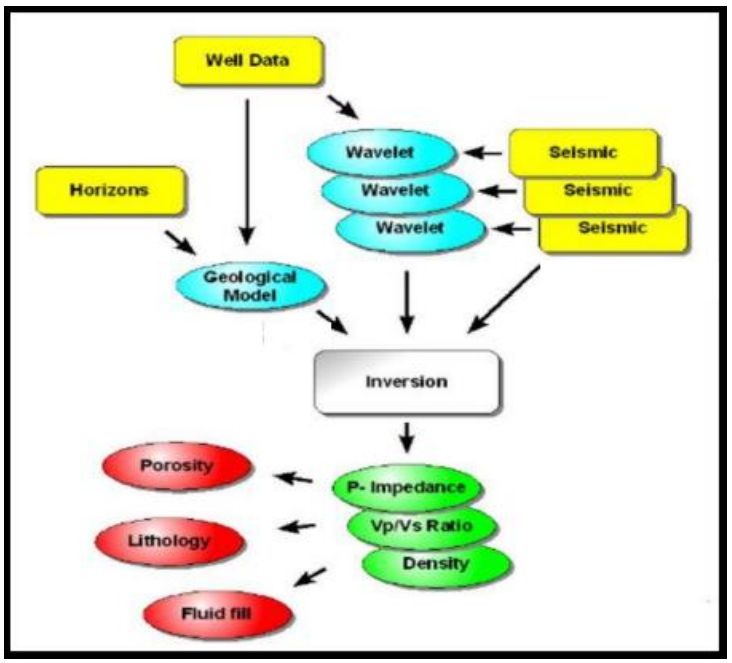

Figure 5.2 Steps adopted for post stack seismic inversion (Sen and Stoffa, 1995).

5.2 Types of Seismic Inversion (Post Stack)

Post stack seismic inversion is usually branched into two main subdivisions named; Deterministic inversion and also the Probabilistic inversion. Deterministic may be further categories into some main subdivisions named; (a) Sparsed spike, (b) Model based and (c) Recursive inversion (Figure 5.3).

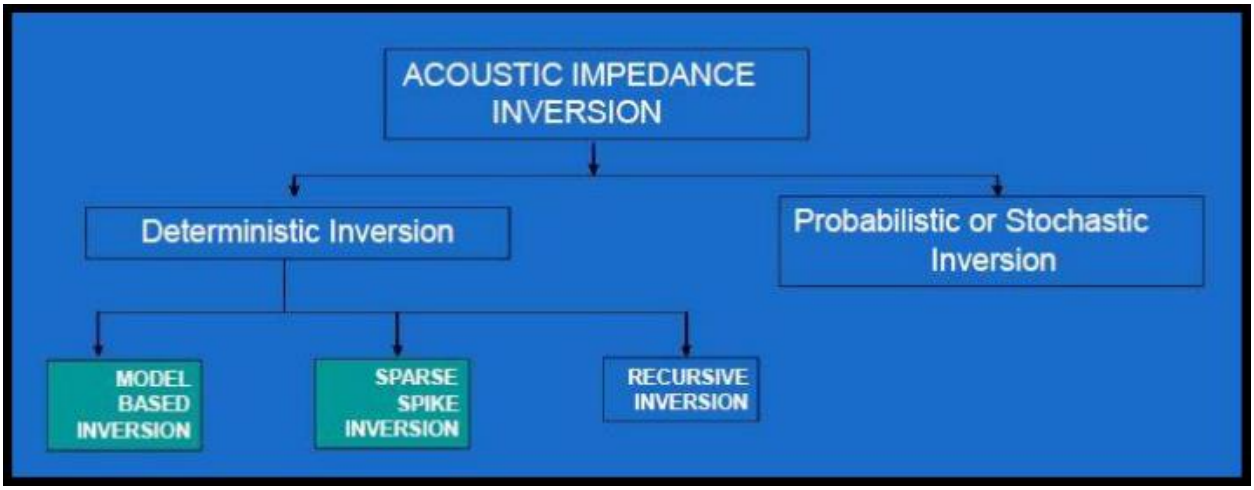

Figure 5.3 Subdivision of acoustic impedance inversion (Veeken and Silva, 2004).

In this chapter, topics for further discussion are Sparse Spike and Model based Inversion. Outcomes of both of these inversion methodologies are analogous however in comparison to model based inversion better results are obtained by Sparse Spike inversion for a whole sparse model, whereas Sparse Spike Inversion yields low resolution as compare to Model Based Inversion when applied to actual data.

5.2.1 Model Based Inversion

The approach used for computation of acoustic impedance of earth is described as seismic inversion. Commonly amplitude mode of seismic data is shown on seismic section which is indeed an interface property however in case of quantitative interpretation of seismic data is executed by applying acoustic impedance which is a layer property.

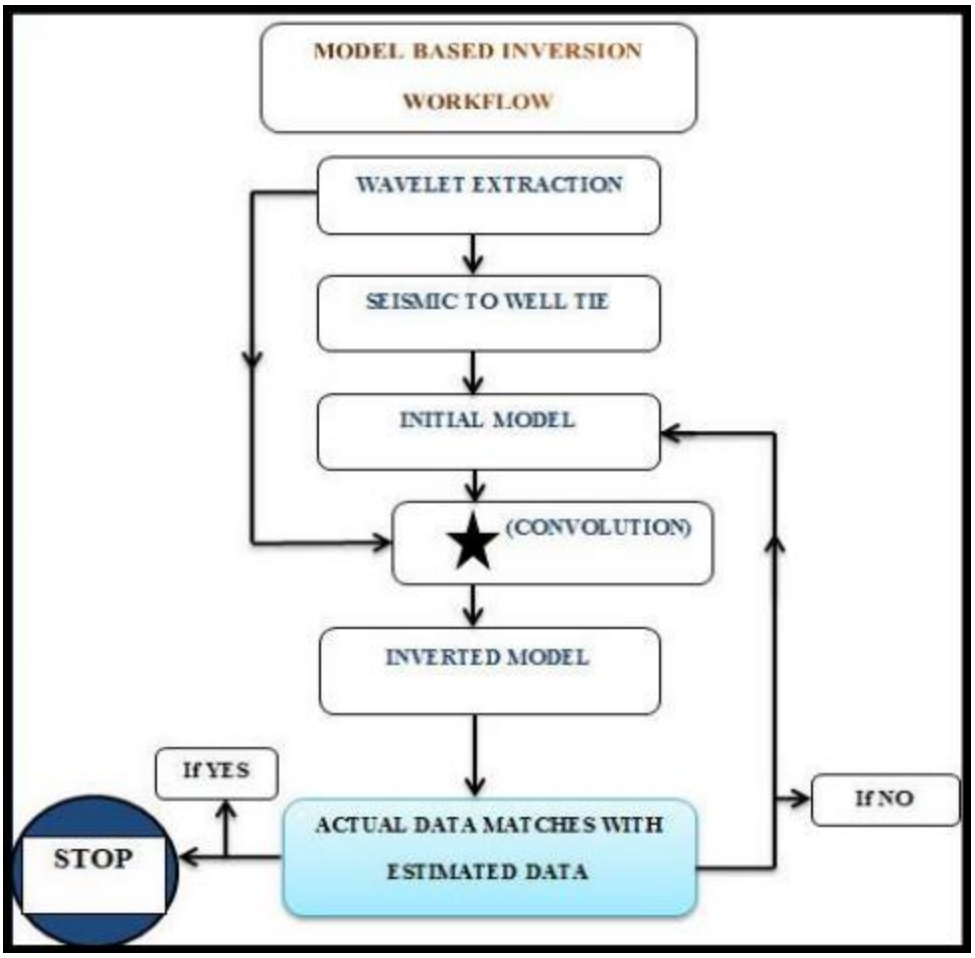

Figure 5.4 Model base inversion workflow for estimating acoustic impedance, porosity and lithology (Kneller at al., 2013).

After estimating impedance, it may be utilize for identifying different properties of reservoir zone such as water saturation, Model Based Inversion is performed u3azsing a general linear algorithm of inversion. Assumptions of this algorithm includes that a known wavelet (W) and seismic trace (S) are incorporated to generate an initial estimated model and modification of this model runs up to a satisfactory level where actual and synthetic trace ties (Gavotti et al., 2014). Simply, the purpose behind alteration of geological model is to minimize the error present between actual and synthetic seismic trace. A reliable model generation is possible from this approach along with a comprehensive grip on geology (Kneller et al., 2013).

(a) Extracting Wavelet

Seismic data is used to extract a constant phase wavelet that is an essential requirement in case of converting seismic data into acoustic impedance and then convolve it with reflectivity

series of seismic section. Thus it is used to carry out correlation between inverted seismic reflectivity at well point and extracted reflectivity. Another important property is the phase of wavelet i.e. it must be in minimum or zero phases in order to have good result for inversion and seismic interpretation. After extracting the wavelet, exact amplitude estimation of wavelet become promising thus inversion based seismic estimates are accurately scaled as compare to real seismic.

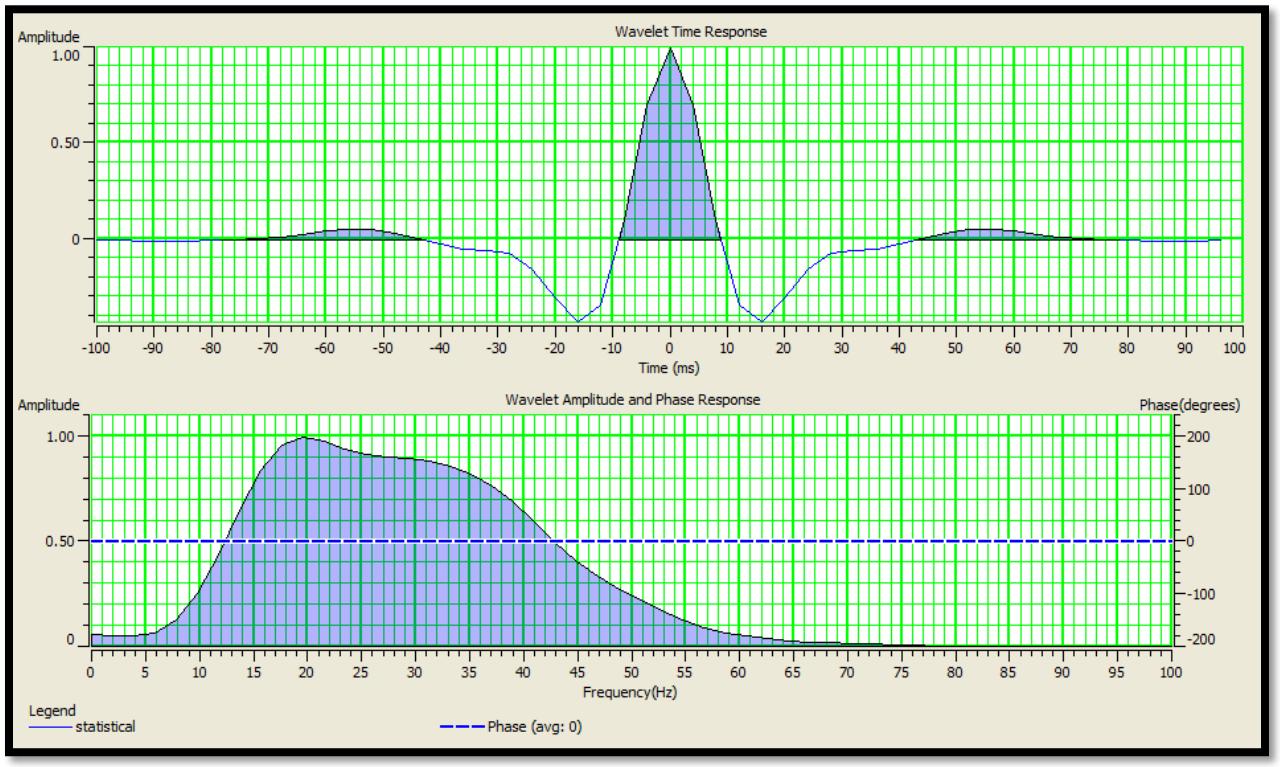

Figure 5.5 Extracted statistical wavelet showing amplitude and phase spectra from seismic.

Inversion results are highly affected by the input wavelet phase shifts i.e. if value of phase shift is high then there will be more chance of error in resulting impedance (Jain, 2013). Its algorithm includes auto-correlation of trace's amplitude spectrums defined on a particular window. Phase response and amplitude spectrum of an extracted wavelet are shown in Figure 5.5.

(b) Well to Seismic Tie

To invert seismic data it is essential to perform well to seismic tie, for this purpose Naimat Basal-01 and Siraj-South-01 is used as a control point. The extracted wavelets are shown in Figure 5.5 is extracted from seismic data present in surroundings of well, is tied to reflectivity series of both wells. 1D forward model is generated for Naimat-Basal-01 well and shown in Figure 5.6.

Inversion accuracy greatly depends on the accuracy of well to seismic tie thus it demands best possible results to minimize errors.

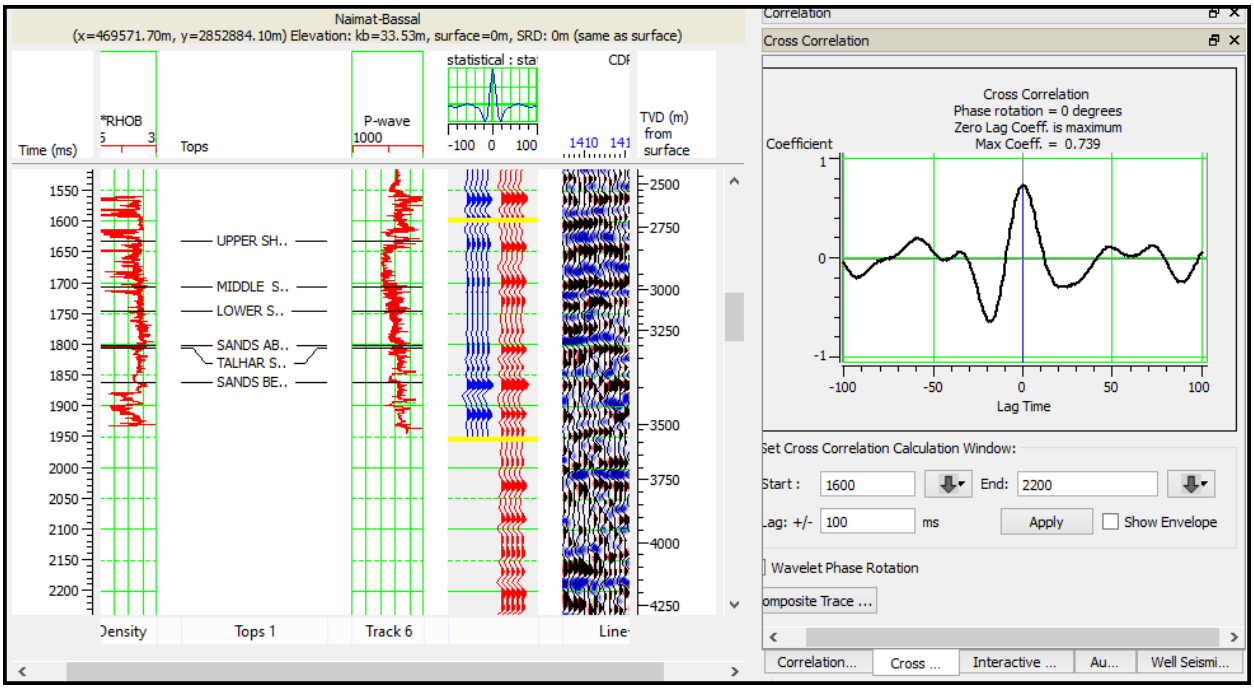

Figure 5.6 Well to seismic tie at well Naimat-Basal-01.

(c) Initial Model With Low Frequency

Acoustic impedance can be described in terms of absolute and relative impedance. In case of relative impedance it is not necessary to generate a model with low frequency however for calculation of absolute impedance; a component with low frequency (between 0 to 10 Hz) is introduced to algorithm used for inversion of amplitudes data (Cooke and Cant., 2010). Introduction of a model having low frequency is needed to reduce problems such as absence of low frequencies in seismic data which leads inversion towards failure in recognizing a thin bed and produce tuning effect due to false amplitudes. Sparse Spike inversion involves separate addition of low frequency model whereas low frequencies addition take place as a part of model Based inversion algorithm. Initial model for model based inversion is shown in Figure 5.7 as an input.

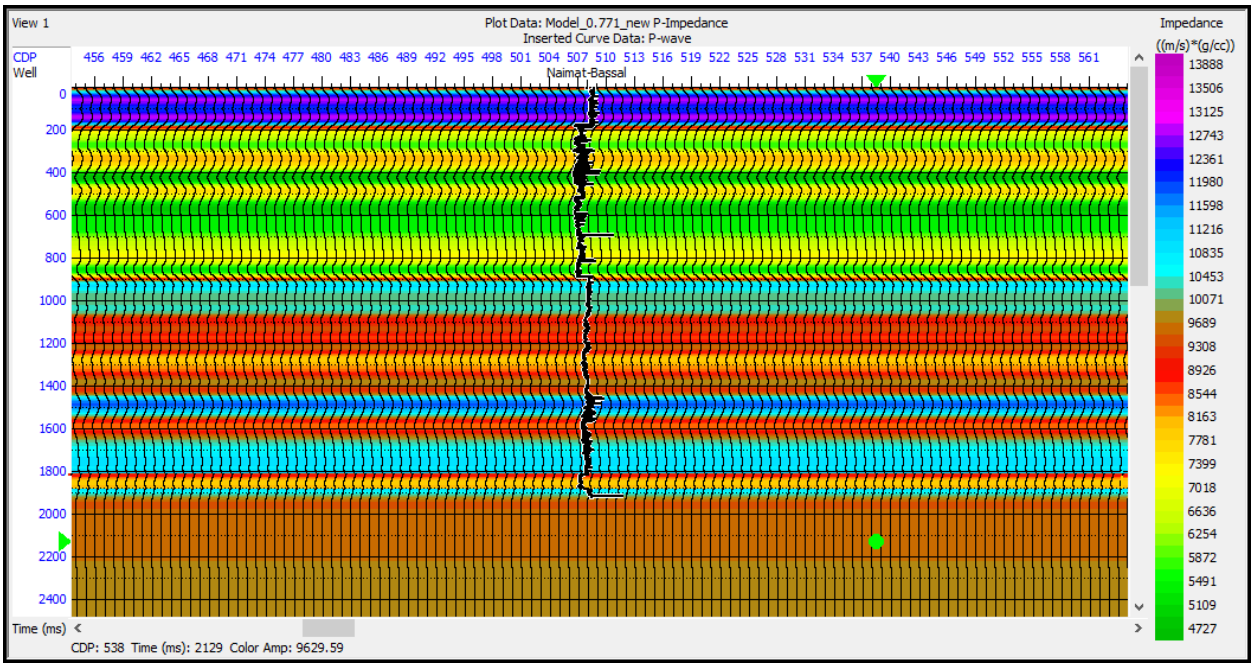

Figure 5.7 Initial Model having Low frequency.

(d) Inversion Analysis

Model Based Inversion analysis is executed at Naimat Basal-01 well point of khipro area. First stage was the extraction of a statistical wavelet having 1600-2200 milliseconds range in time window. A comparison between synthetic trace and inverted trace at well site is necessary to adjust extracted wavelet frequency range. Value of correlation coefficient "r" is showing good results and obtained from correlation of black seismic and red synthetic traces. Correlation between well data and seismic data is 0.98 as shown in Figure 5.8. Root mean square error values is 0.16. Overlapping of both inverted as well as actual impedance depicts that inversion results will be trustworthy. Model Based Inversion results are displayed in Figure 5.8 for seismic line KH2000-08. Particular time window from 1600 to 2200 milliseconds is used to perform inversion analysis with aim to detect target horizon existing in zone of interest. Outcomes of inversion are the colorful displays of several bands, showing different acoustic impedance value for every single stratum. The zone of interest contains formation such as sand below Talhar shale which exist between 1600 to 2200 milliseconds time window. Different colors on color bar shows variations of inverted impedance where yellow and green color represents low impedance value while high impedance is characterized with magenta and blue colors. In case of shaly sand comparatively low

impedance response is regarded as reservoir zone thus layers with yellow or brown color at approximate time zone i.e. 1870 milliseconds indicates the reservoir zone.

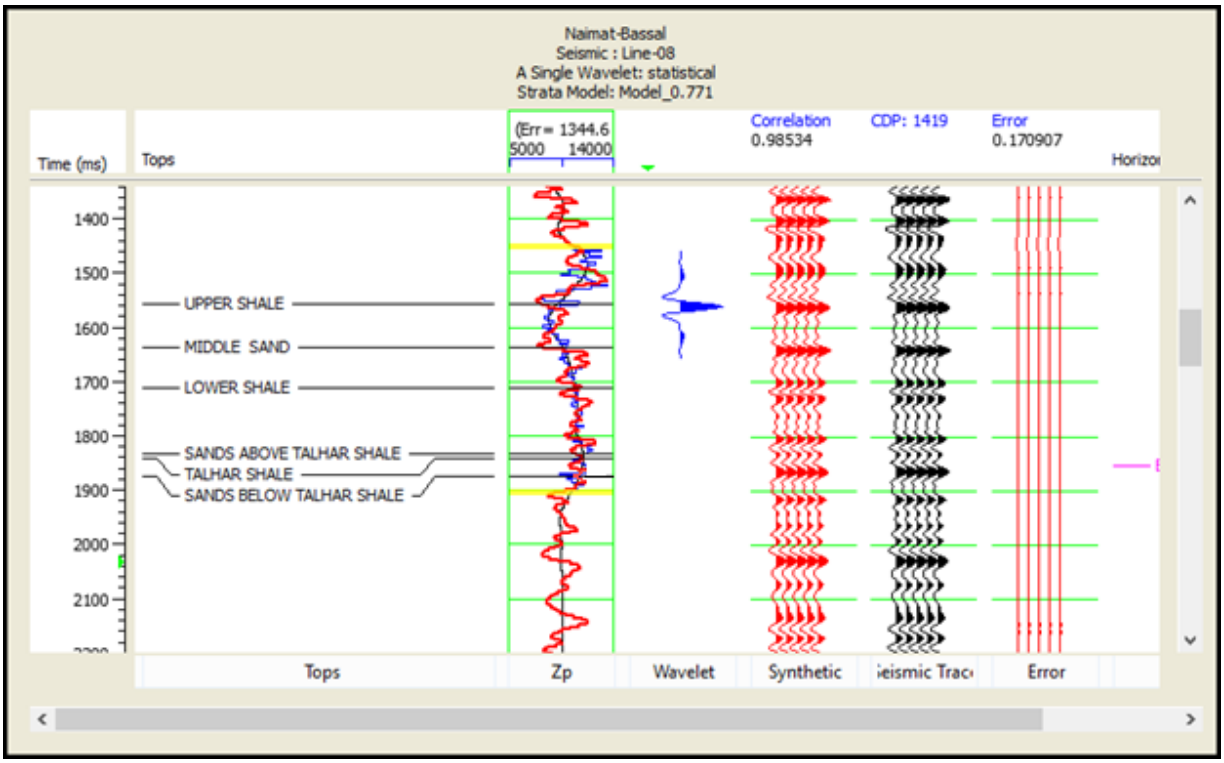

Figure 5.8 Post Stack Seismic inversion analyses (Model based) at Naimat-Basal-01

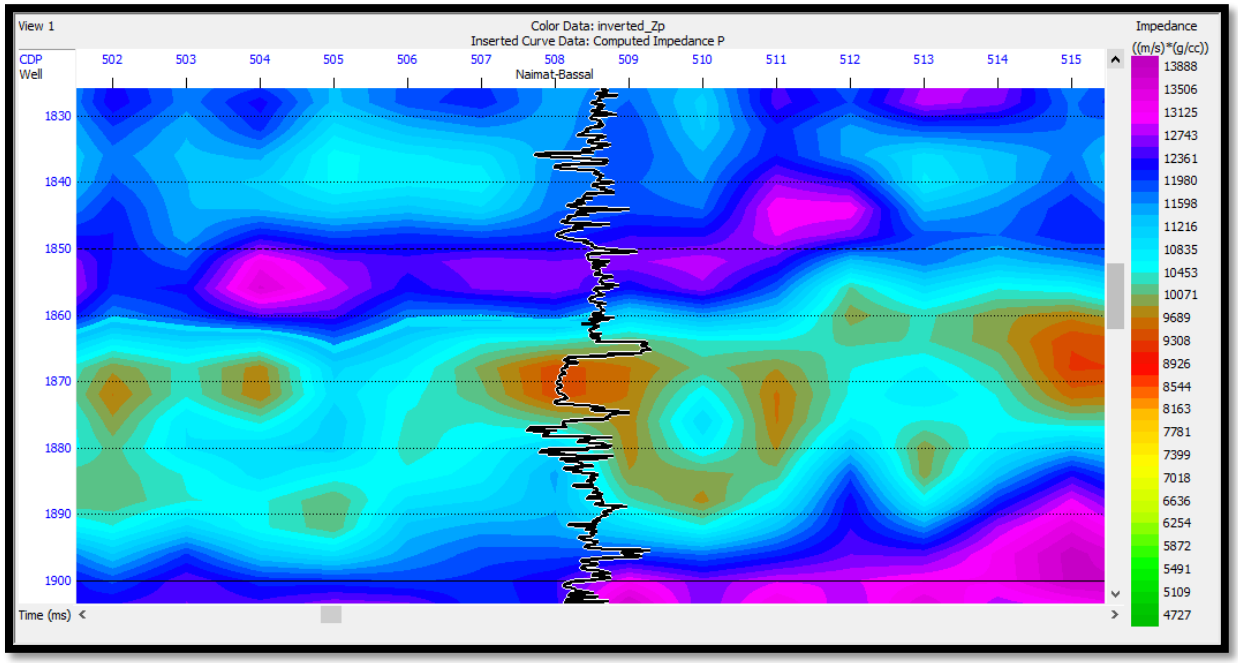

Figure5.9 (a) Cross sectional view of Low impedance zone of line 2000KH-08.

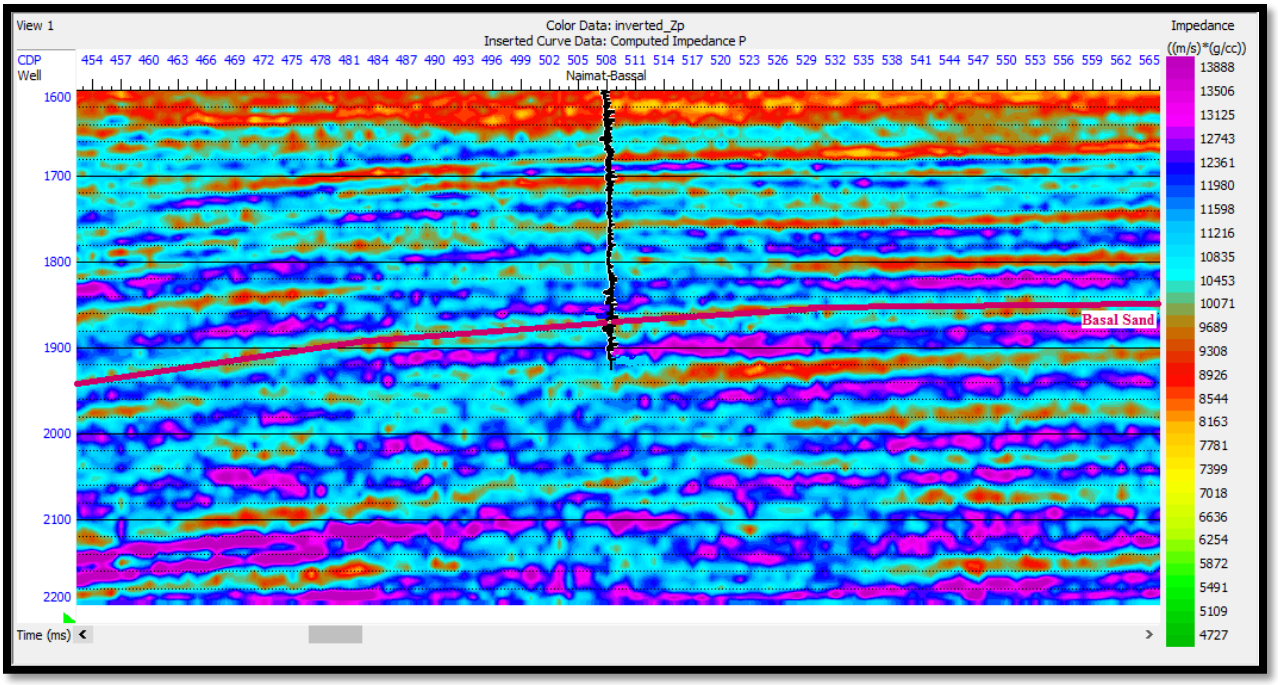

Figure 5.9 (b) Cross sectional view of inverted impedance of line 2000KH -08.

Well location is the control point in a seismic survey. It is also visible that moving away from the well along dip or strike direction result in loss of well control, Basal sand cannot easily be recognizable as it has poor continuity on seismic.

5.2.2 Sparse Spike Inversion

Sparse Spike Inversion makes use of linear programming seismic attribute for this study work. Formations tops, well logs and seismic 2D data was loaded in a project of Hampson Russell software. Density (RHOB) and sonic logs (DT) were incorporated to calculate impedance log and after inverting this impedance log a reflectivity series was generated. Process of convolution takes place between the wavelet extracted from seismic and reflectivity series in order to make an inverted synthetic trace. Inverted synthetic trace is correlated with actual trace several times to achieve best fit match. To build a priori model, both geological tops and impedance logs are required moreover interpolation and extrapolation of impedance logs is carried out to find best fit model (Ali et al., 2018). Figure 5.10 shows result of inversion analysis which was carried out for Naimat Basal well using extracted and synthetic traces, which gives 0.99 value of correlation coefficient. Matching between curves of inverted impedance and impedance log is up to an acceptable level to produce inverted volume.

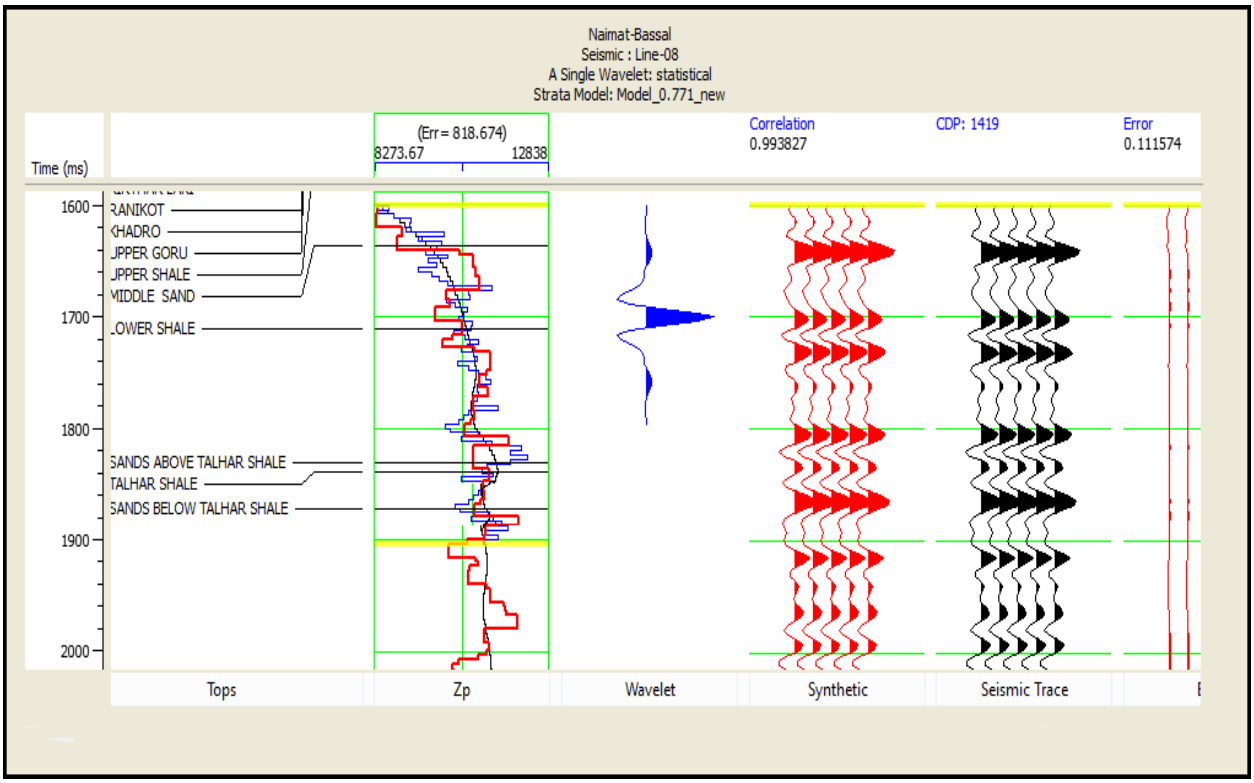

Figure 5.10 Results of Sparse Spike inversion analysis.

Inverted section from Sparse Spike Inversion is shown in Figure 5.11 for Naimat Basal well present on seismic line 2000KH-08. This result is generated by using algorithm for sparse spike inversion so as to invert the 2D seismic data. Cross sectional view of impedance log is presented at well position showing inverted impedance. Small impedance value got detected at time 1880ms showing Basal Sand through light brown color, impedance from 9308-10071 (m/s)*(g/cc) specifically for mentioned layer. Small acoustic impedance categorized the gas reservoirs (Ibrahim, 2007). Quality gas reservoir's impedance values ranges from 7900-10050 (m/s)*(g/cc). Shales are categorized by high impedance values (Gavotti, 2014). Relative to model based inversion, sparse spike inversion has lesser resolution in ultimate impedance results.

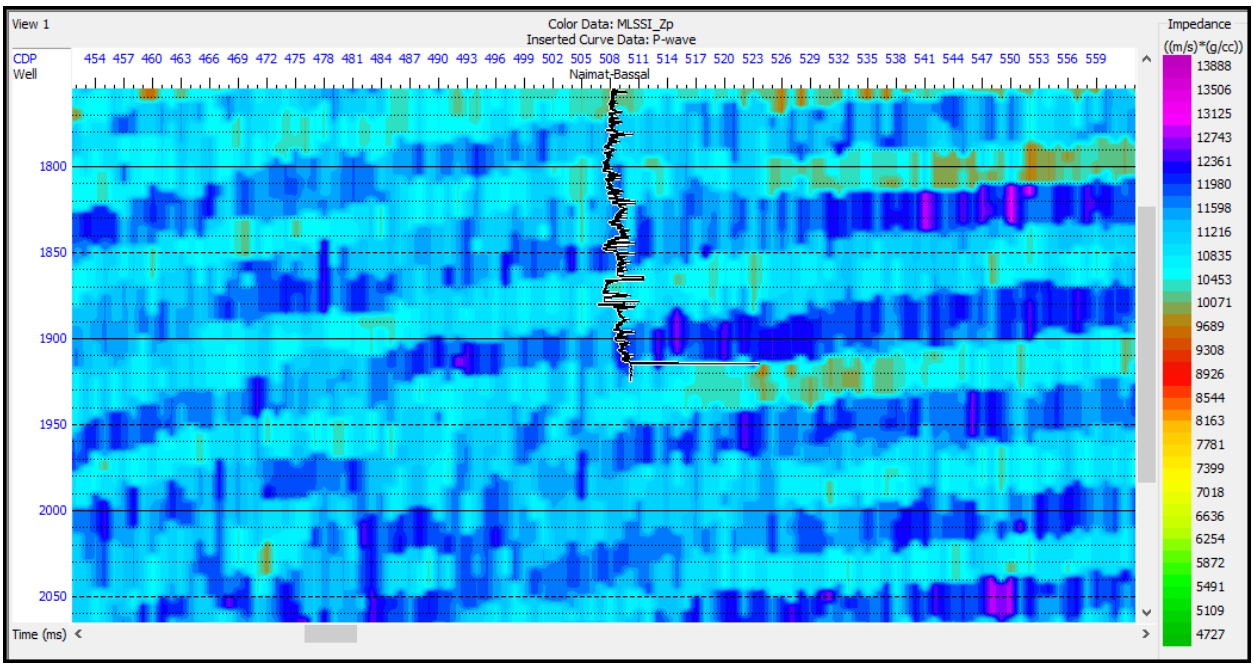

Figure 5.11 Inverted section of line 2000KH-08 at Naimat-Basal-01.

5.3 Comparison of Model Based and Sparse Spike Inversion:

A comparison can be drawn between sparse spike and model based inversion for this specific research study. It is concluded that analogous results of inverted data using model based inversion provide high accuracy and reliability as compare to sparse spike inversion, however in case of a whole sparse model, accurate and reliable results are achieved through sparse spike inversion. Sparse Spike provide better results at different intervals but in Figures 5.12 and 5.13, it is observed that sparse spike inversion algorithm cannot resolve layer of Basal Sand as resolved by model based inversion. Amount of error encountered in sparse spike inversion exceeds the error values of model based inversion. Other significant parameters which can be calculated from inversion are porosity, velocity and density besides inverted seismic data which is major target of inversion. Both velocity and density incorporate to produce impedance hence impedance provide a rough judgement of these attributes.

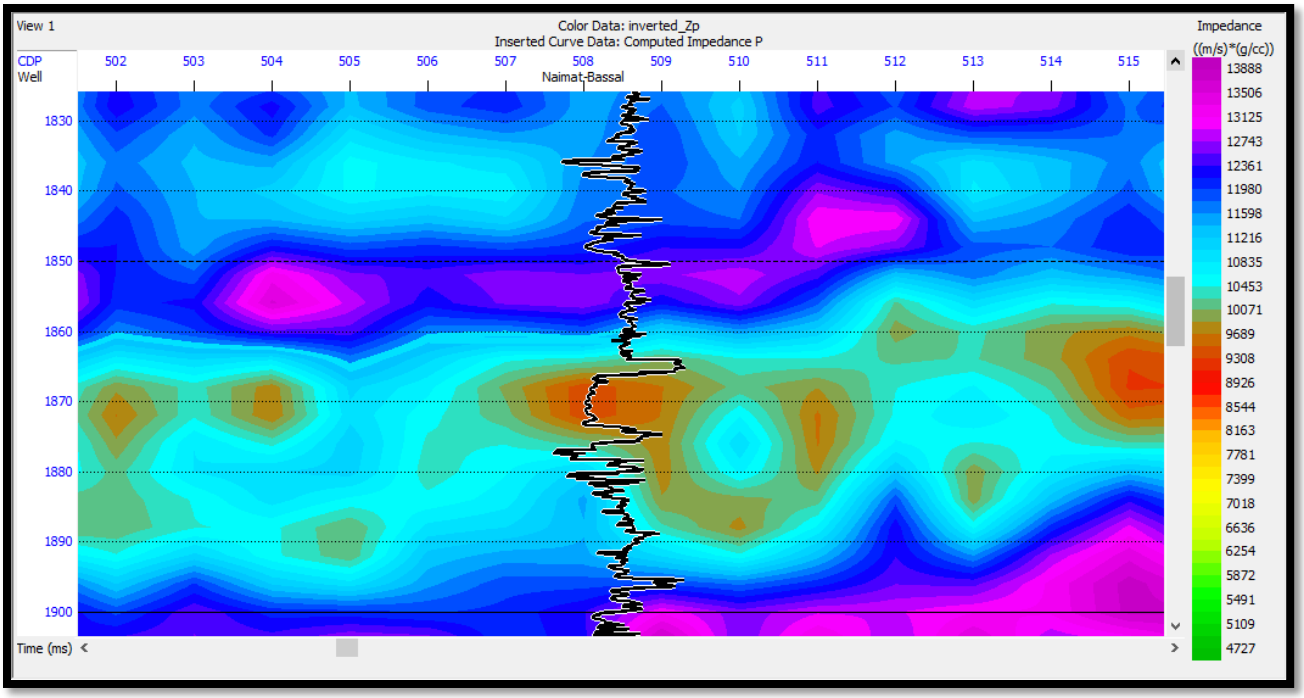

Figure 5.12 Model based inversion.

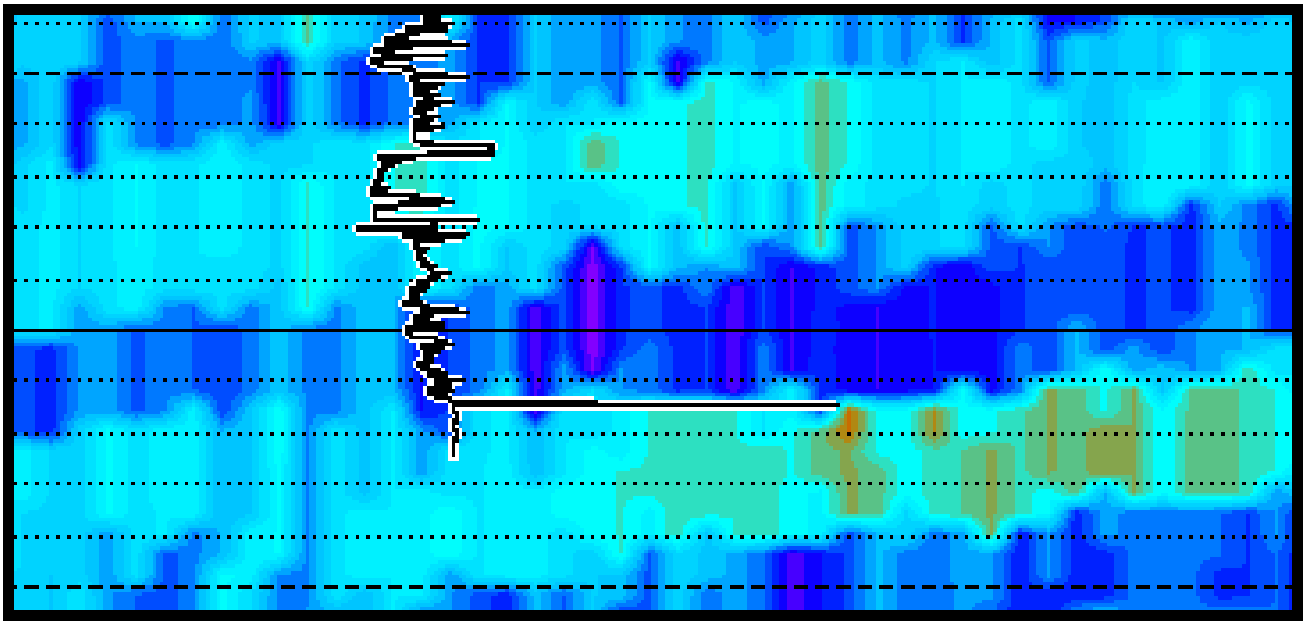

Figure 5.13 Sparse Spike inversion.

CHAPTER 6

PORE PRESSURE PREDICTION USING WELL DATA

6.1 Introduction to Pore Pressure

In order to drill oil and gas well seamlessly and cost-effectively precise estimation of pore pressure and fracture gradients is required (Eaton, 1969). It involves investigation of the overpressure zones, considered to be most crucial one (Sayer et al., 2002). An efficient drilling plan requires awareness of the formation pressures that allows designing an effective mechanism to better control a well during drilling (Sayer et al., 2002). The importance of precise estimation of the formation pressure and fracture gradients can be viewed by the fact that the drilling program is tailored to safely monitor the pressure variation to prevent blowouts (Bruce and Bowers, 2002). The aim of this chapter is to analyze the pore pressure variations in the study area on well data by using Eaton and Bowers methods. The pore pressure prediction results will be useful for future drilling programs in the study area. This chapter provides background information pertaining to Pore Pressure prediction techniques. Precise attempt is made to use definitions and explanations most extensively accepted and in normal usage among professionals linked to pore pressure within the oil and gas industry. The chapter starts with some basic terminologies commonly used different mechanism which causes the overpressure mechanism in subsurface. Later this chapter develops different pore pressure prediction techniques and then finally these techniques are applied on study area to develop a pore pressure model from seismic and well data in study area. Figure 6.1 describes the some basic terminologies which are commonly used in pore pressure estimation techniques.

6.2 Hydrostatic Pressure

The pressure applied by static column of fluid at any depth is referred as hydrostatic pressure. This is dependent on formation fluid density (water or brine), and vertical height of the fluid column. Hydrostatic pressure usually calculated by (6.1).

$$P_h = \rho g H \tag{6.1}$$

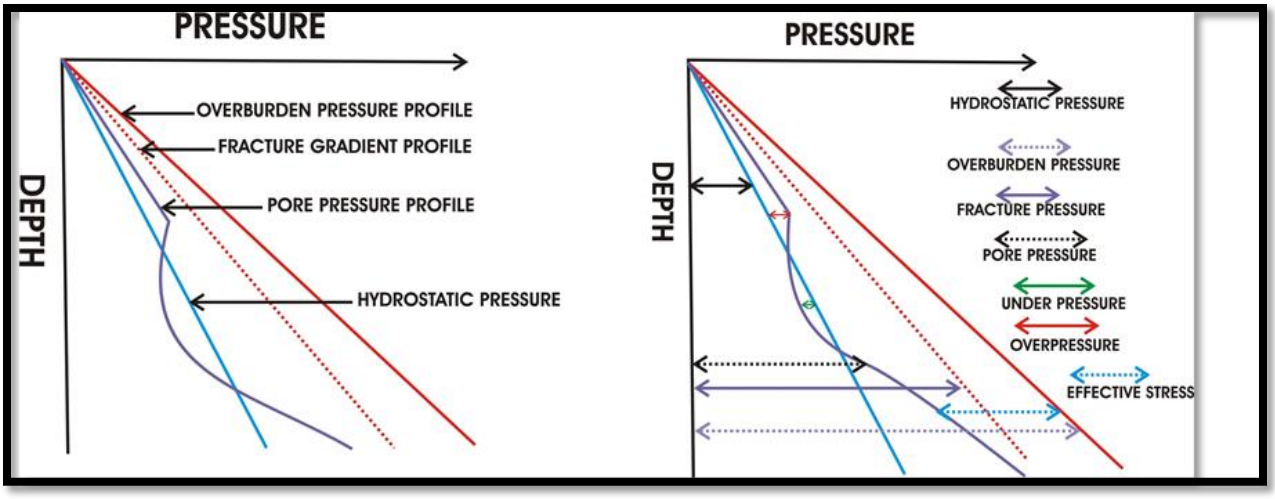

Figure 6.1 Basic terminologies used in Pore Pressure (Nwankwo, C.N. and Kalu, S.O. 2016).

Here P_h denotes hydrostatic pressure, ρ is average density of liquid, g is acceleration due to gravity, and H is perpendicular height of water column. Hydrostatic pressure gradient is rate of change of pressure with depth dP_h/dH, and calculated as in equation (6.2)

$$dP_h/dH = \rho g \tag{6.2}$$

For this study, average water density value of 1.037 g/cc and hydrostatic pressure gradient 0.465 psi/ft is used.

6.3 Overburden Pressure

The overburden (or Lithostatic) pressure is the pressure exerted by the weight of overlying sediments and contained fluids and is the total vertical stress S_v utilized in the Terzaghi equation. Lithostatic pressure is expressed by (6.3)

$$S_v=\rho bDg \tag{6.3}$$

Here S_v denotes the lithostatic pressure, ρ is the average bulk density, D is the vertical depth from datum (sea floor for offshore and land surface for onshore), g is the gravitational constant.

6.4 Pore Pressure (Pp)

Pore pressure/Formation pressure is defined as the stress delivered by the fluids seated in the pores. An indirect method to predict Pore pressure is to compare the normal (expected) and actual curves responses of sonic, neutron, density, or resistivity logs.

6.5 Normal, Over and Under Formation Pressure

The pore pressure profile equal to the hydrostatic pressure profile referred as normal formation pressure. The Pore Pressure which is higher than hydrostatic pressure is referred as overpressure, it is the zone where formation pressure P_p is higher as compared to hydrostatic pressure P_h. It equals the excess pressure OP expressed mathematically in equation (6.4)

$$OP = Pp - Ph \quad (6.4)$$

Identification of over pressured zones is essential for designing a drilling plan. The Pore Pressure which is lower than hydrostatic pressure is referred as under pressure. Usually production from reservoir depletes its pressure thus causing the generation of under pressure zone. (Osborne and Swarbrick, 1997).

6.6 Vertical Effective Stress

It is the measure of difference of overburden pressure S_v and the formation pressure P_p. Since there is no direct way to estimate vertical effective stress σ_v so estimation is made utilizing Terzaghi's equation (Terzaghi, 1943). Mathematically expressed as:

$$\sigma_v = S_v - P_p \quad (6.5)$$

6.7 Pore Pressure Prediction

One of the key concepts required for pore pressure prediction is an understanding of the relationship between compaction, porosity and the associated stresses during the burial of sediments (Swarbrick et al., 2001). All of the standard methods e.g. Eaton method and Bowers method are based on this concept.

6.8 The Normal Compaction Trend (NCT)

Defining a normal compaction trend is one of the key stages in pore pressure prediction. The Terzaghi equation (Terzaghi, 1943) describes the relationship between total stress S_v, pore pressure P_p and effective stress σ, which for extensional basins is normally rewritten in terms of vertical stresses as equation (6.6)

$$S_v - P_p = \sigma_v \quad (6.6)$$

The sediments which are compact normally their porosity is reduced at the same time as pore fluid is expelled (mechanical compaction). During burial, increasing overburden is the prime

cause of fluid expulsion. If the sedimentation rate is low, fluids within the pore space can escape resulting in normal compaction. If this is the case then, porosity decreases at a predictable rate with increasing depth, referred to as the Normal Compaction Trend (NCT) (Dutta, 2002; Bowers, 1995).

As the overlying burden increases the rock compacts and causes porosity to reduce. Sediments compact under the load of overlying deposits and the porosity decreases.

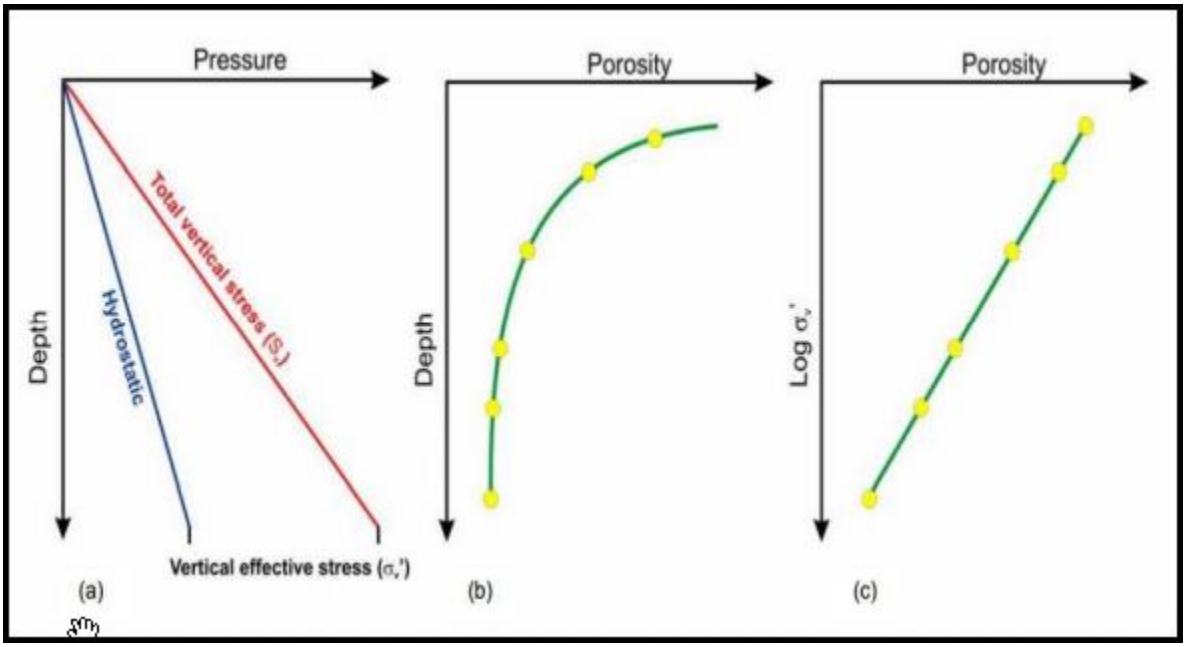

Figure 6.2 (a) Normally pressured sediments gradient will lies on hydrostatic profile in pressure depth profile (b) Porosity decreases with depth for normally compacted sediments in a predictable manner (c) Normal compacted sediments produces a straight line in porosity effective stress profile (Swarbrick, 2012).

If it is assumed that porosity is a proxy for vertical effective stress (i.e. low porosity = large amount of compaction = high vertical effective stress and vice versa) and some prediction can make how porosity will change with changing vertical effective stress then a means of relating porosity to pore fluid pressure is available (Harrold et al., 1999) . By rearranging the Terzaghi equation (Terzaghi, 1943) it is possible to estimate the pore pressure in shales if the total vertical stress and effective vertical stress are known/ estimated.

$$P_p = S_v - \sigma_v \quad (6.7)$$

This is the basic equation which is used for pore pressure prediction for different methods. The total vertical stress (Sv) at any depth is determined from the lithostatic gradient. The most

difficult part of pore pressure prediction is to estimate vertical effective stress (σv), which comes from a response to changes in shale porosity. In normally compacted shale, the magnitude of vertical effective stress increases and porosity decreases (Figure 6.2 (a) & (b)). By defining a normal compaction trend (NCT) within the shales comparisons may be made between the porosity expected if the rock is normally pressured and compacted, and the measured porosity from the well at the depth of interest. Only thick shale sequences can be utilized in this way (Sayers et al., 2002).

6.9 Disequilibrium Compaction

In fine grained sediments such as muds and shales, fluids may not be able to escape effectively due to very low permeability unlike sands, and the pore fluid assumes more of the stress than for a normally compacted rock at the same depth. The weight of the overlying sediment is transferred from the grains to the pore fluid (Harrold et al., 1999). This situation is referred to as Disequilibrium Compaction or under compaction and leads to a lower vertical effective stress acting on the rock than would be observed in a normally compacted rock at the same depth (Terzaghi, 1943; Osborne and Swarbrick, 1997).

The depth at which disequilibrium compaction occurs, i.e. the point at which fluids are no longer being expelled effectively due to low permeability as the rock attempts to compact, is referred to as the top of overpressure (Tingay et al., 2009).

6.10 Pore Pressure Prediction Methods

There are two main methods commonly used to determine pore pressure where overpressure is due to disequilibrium compaction.

1) Eaton's Ratio Method (Eaton 1972) which is an empirical methodology.

2) The Bowers Method which is an empirical methodology.

Assumptions:

These methods are devised assuming number of assumptions. The assumptions considered are illustrated as under (Zhang, 2011; Osborne and Swarbrick, 1997)

- The rocks are mechanically compacted and the predominant origin of overpressure is related to disequilibrium compaction.

- The rocks are presently at their maximum effective stress (likely to be their maximum depth of burial).
- The predominant lithology is thick shale sequences. The greater porosity and permeability in sands means that they can be affected by processes that transfer pressure into or out of the system therefore they have to be dealt with separately
- The Normal Compaction Trend can be defined
- The measured log value or velocity can be compared with either the value on the NCT at the same depth (Eaton), or at a shallower depth with the same log value/porosity, and assuming the same porosity = the same effective stress (Equivalent Depth)
- Shale porosity can be well imaged (e.g. using interval velocities, petrophysical or drilling parameter).
- Pore pressures can be determined with reference to a well constrained overburden (lithostatic stress).

Both Eaton and Bowers methods utilize the relationship between total vertical stress S_v determined from the overburden and vertical effective stress σ_v which is determined from porosity (or a proxy for porosity e.g. sonic or resistivity log or seismic interval velocity data).

6.10.1 Eaton Ratio Method

One of the most commonly used approaches for relating porosity to pore pressure is Eaton's Ratio Method (Eaton, 1969, 1972). The Eaton Ratio Method uses the ratio of the recorded value of a porosity related measurement (e.g. sonic or resistivity) to the value of that measurement on the normal compaction curve to estimate the vertical effective stress. The value of the measurement ratio is raised to an exponent, the value of the Eaton exponent is based on matching empirical data with outputs from the formulae using a variety of exponent values. The value of the exponent may be varied, to calibrate to local data. The default exponent value for sonic and velocity data is 3.0 and 1.2 for resistivity (Chopra and Huffman, 2006; Hermanrud et al., 1998).

The equation used in Eaton Method for V_p log is

$$P_{Pore} = P_{Litho} - VES \quad (6.8)$$

Here $VES = (P_{Litho} - P_{hyd})\,[V_p/V_n]^3$, V_n is Velocity on Normal Compaction Trend at corresponding depth where Plitho, Phydro and V_p value has been taken.

6.10.2 Bowers Method

Bowers (1995) method uses the velocity and empirically determined parameters to calculate the vertical effective stress, which is subtracted from overburden to get pore pressure. Method is based on assumed empirical relation between vertical differential stress and the velocity:

$$V = Vo + A\sigma B \quad \text{or} \quad \sigma = ((V-Vo)/A)*1/B \tag{6.9}$$

Where, Vo is the velocity of mud-line (unconsolidated fluid saturated sediments), and A and B describe the variation in velocity with increasing differential stress.

6.11 Pore Pressure Prediction Workflow From Well Log Data

Pore pressure prediction using methods under study can be drawn into a workflow representing the study scheme in Figure 6.3.

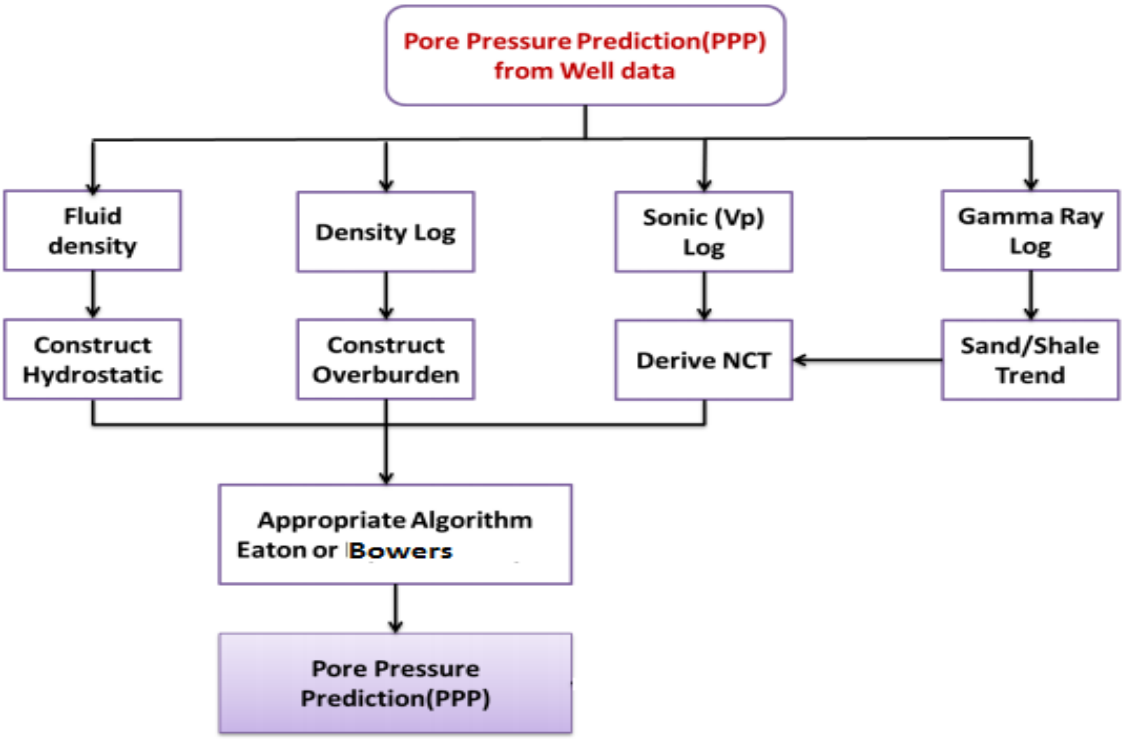

Figure 6.3 Generalized Workflow of Pore Pressure Prediction from Well logs data.

6.12 Well Based Pore Pressure Prediction

Interval velocity derived from sonic log is used for estimation of pore pressure. Both Eaton and Bowers methods were used for this purpose. Below mentioned sequence is for pore pressure analysis based on well:

(a) Distinguishing Shale Packages on the Lithology track (Using Gamma ray with cutoff of >35Api)

(b) Computing the Shale Points (once demarcation of shale packages is done, shale points were Evident in more logs)

(c) Refining of Shale Points using velocity representing dataset (Velocity values chosed at these point where GR >>35Api, dispersed data set is diminished)

(d) Computation of Overburden Gradient (computed using density data from surface till depth)

(e) Calculating a Normal Compaction Trend Curve (computed by passing a line from these Shale Points for velocity curve and using bower's method)

(f) Executed the Pore Pressure Prediction Analysis

6.13 Results and Analysis:

Figure 6.4 shows the pore pressure prediction sequence for Naimat-Basal-01 well. In first track Gamma ray (filtered using simple boxcar method, weighted 65) is shown with straight lines known as shale base line, in second track interval velocity in ft./s (calculated from sonic) is displayed, third track showing the normal compaction trend (NCT) having unit of μs/ft. and in last track hydrostatic pressure (HSP), over burden gradient (OBG) which is computed from density log (missing values were found using Gardener relation) and predicted pore pressure (PP) of both the Eaton and Bowers method are displayed, all the curves in last track have the same unit i.e. psi.

Interpretation of predicted pore pressure showed that Eaton and Bowers curves produces almost similar results and no pronounced variation found between both of them. Figure 6.4 clearly

showing the pore pressure condition of well, upto 1400 m the formations shows slightly over pressured then afterward till 2800m depth all the formations are under pressured or in normal pressure. After 2800m to 3080m thick upper shale sequence which (might be acting as seal) is over pressured, values ranging from 4000psi to 6200psi Figure 6.5. Identification of this over pressured shale is very crucial because if its pressure is not calculated correctly then well will be blown out causing damage to environment as well as infrastructure. Prediction of pore pressure in already drilled well will help us to maintain pressure and minimizing the chances of blow out while drilling the exploratory wells in the vicinity of these wells. Below the upper shale sequence at depth of 3080m to 3480m Talhar shale is also over pressured values ranging from 5000psi to 5750psi but its magnitude is less than the seal, basal sand reservoir is almost within the normal pressured condition and slightly under pressured.

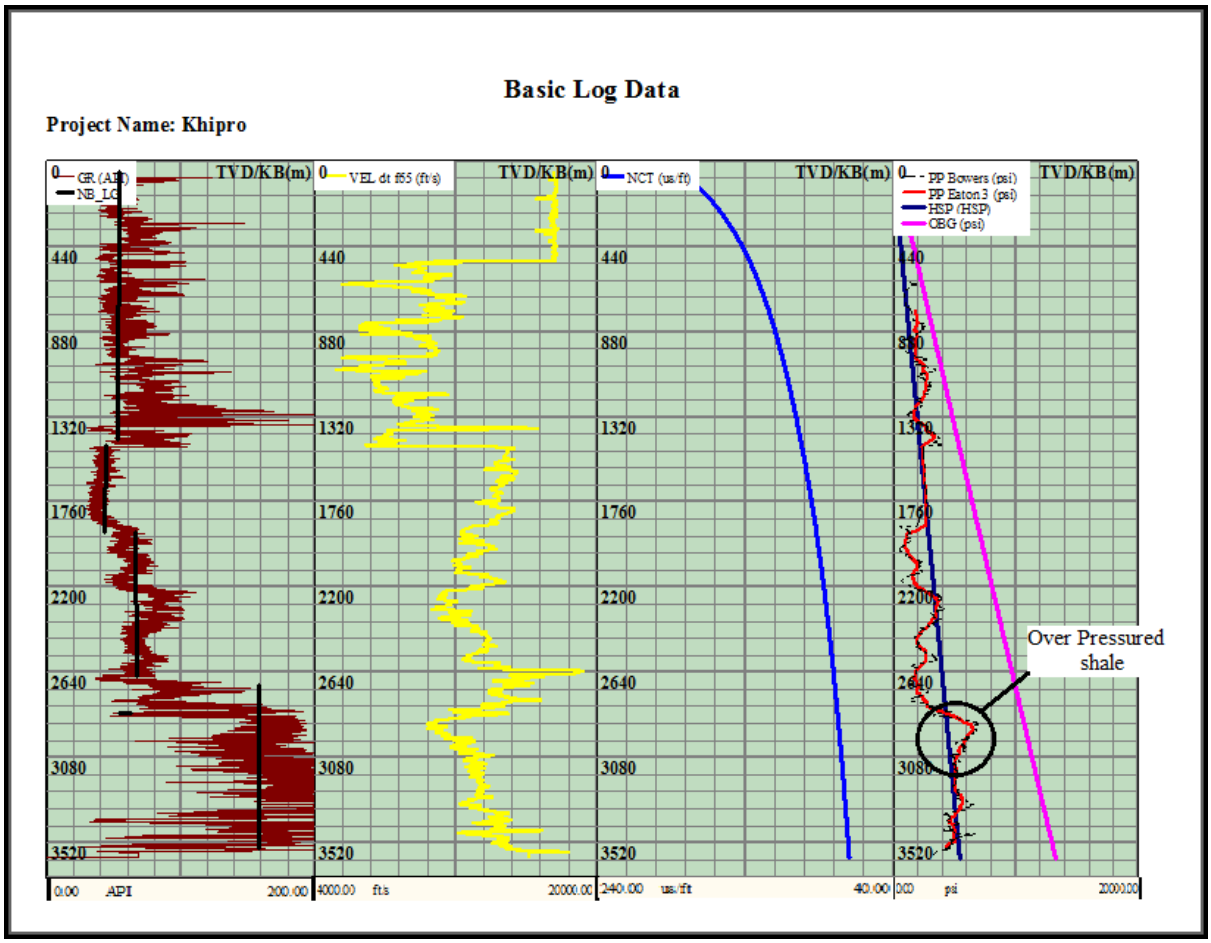

Figure 6.4 Pore pressure prediction sequence for Naimat-Basal-01 well.

Since pressure data for one well have been identified and computed the parameter for the pore pressure now by using them on another well i.e. Siraj-South-01 and compute the pore pressure. Figure 6.6 shows the pore pressure prediction sequence for well Siraj-South- 01. The sequence is almost similar to Naimat-Basal-01 well and we will not discuss it in detail. This well have depth up to 3200m. The reason for pressure prediction in this well was to analyze the abnormal pressure conditions in deeper sands, which are actually gas producing. In this well all the formation are in hydrostatic condition or under pressure but the behavior at basal sand level i.e. at depth of 2900 to 3200m where pressure is slightly lower same as for shallow sands. Upper shale in Siraj-south is not very much above the hydrostatic curve as compared to Naimat-Basal-01 well and the reason might be the difference in thickness of shale bed in both wells location.

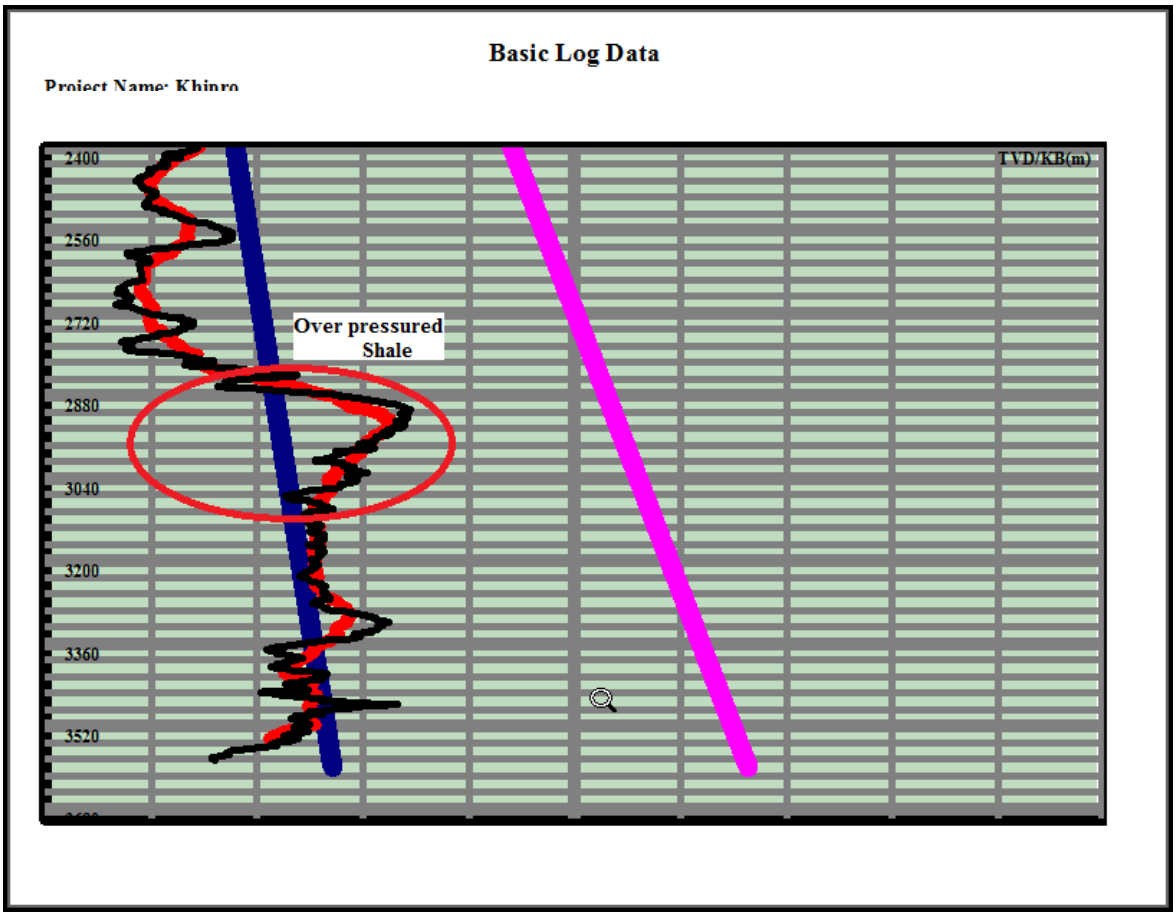

Figure 6.5 Over pressured shale sequence of upper Goru formation in Naimat-Basal-01 well.

6.13.1 Low Pressure Generation Mechanism

The reason for these low pressure needed to be understood, as described earlier this low pressure could be due to low water influx from nearby river or could be due to tectonic unloading erosion. As the area is intensely faulted, each fault block is isolated and there is no sign or rivers for hundreds of Km away, the reason due to water influx has to be dropped. According to research and analysis of geology from cretaceous age to recent for this area, it shows that the formation was deposited in early cretaceous age and during late cretaceous there was rifting associated with

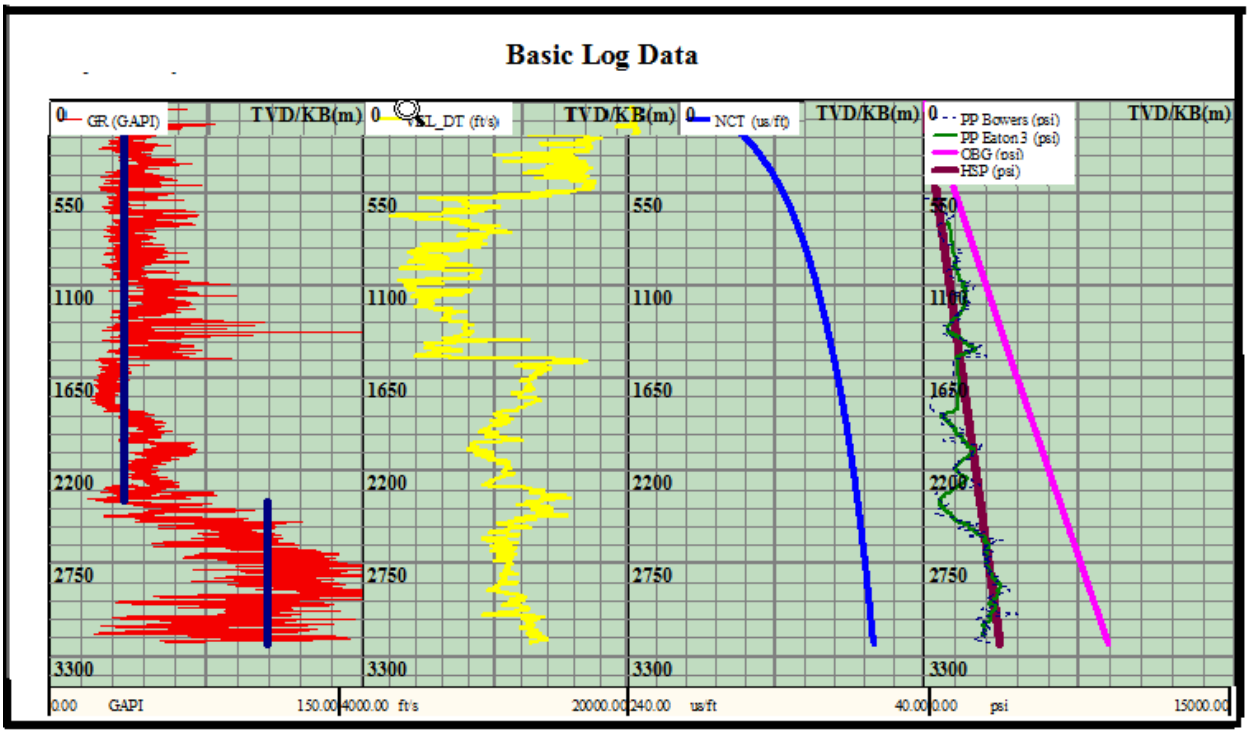

Figure 6.6 Pore pressure prediction sequence for Siraj-South-01 well.

breaking of Indian plate with Madagascar, which stemmed in uplift, erosion, extrusion of the Deccan flood basalts. This reservoir containing either gas or oil were isolated and was subjected to uplift and erosion, the removal of overburden stress caused an elastic rebound of the solids which results as increase in volume of the pores. The elastic dilation of sandstones is about 7×10–6 volumes/psi (Dickey and Cox, 1977). Water expands only 3×10–6 volumes/psi which means that the pressure of the pore water in the aquifer and the enclosing shale's will drop and maybe draw some of the water out of the aquifer.

6.13.2 Overpressure Generating Mechanism

The cross plot of V_p and RHOB for both the studied wells are shown in Figure (6.7), these plots shows that the primary overpressure generating mechanism is might be due to the disequilibrium compaction of sediments (Figure 6.7). Deviation or scatterenes of data from best fit line is very much pronounced which indicates that the disequilibiruim in sediments is not the only phenomena which generates the over pressured formations, the secondary process which might be the reason for over pressured formations is diagenesis of clay or shaly content within the sand formation. These other overpressure generating mechanisms are clay diagenesis and fluid expansion etc. and they are not evident in the studied wells.

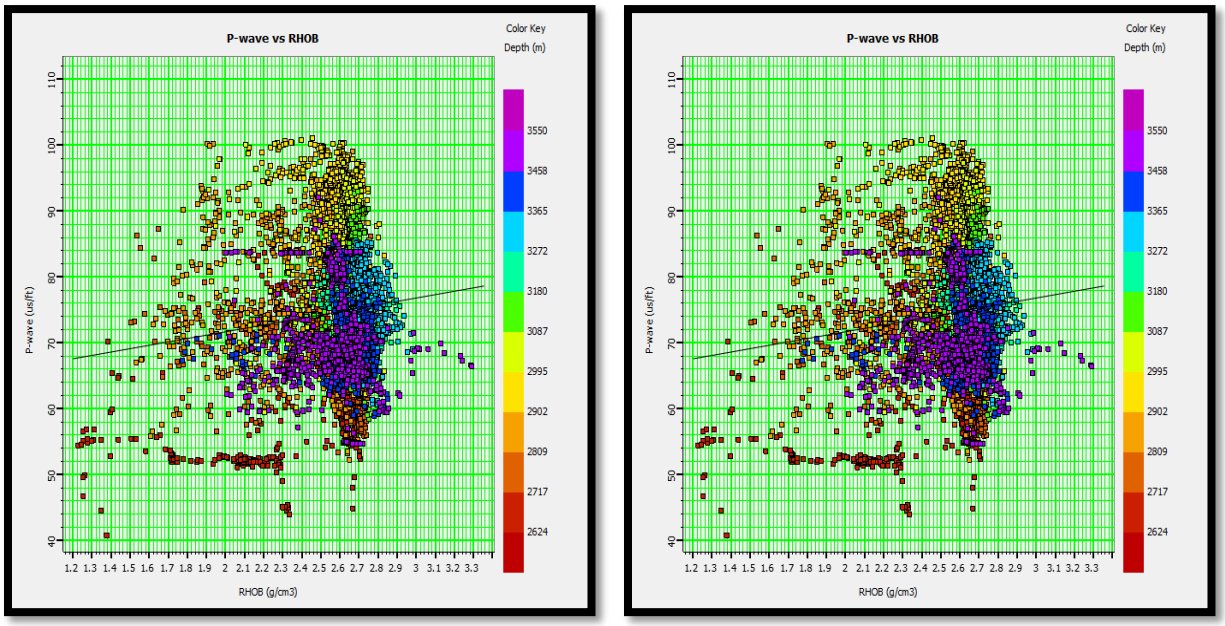

Figure 6.7 Cross Plots between Density and velocity for Naimat-Basal-01(left) and Siraj-South-01(right) wells, along the regression line data points showing the pressure due to disequilibiruim and the diversified points are indicating the pressure generated due to other mechanisms such as diagenesis of clay or expansion of fluid.

6.14 Prediction of Pore Pressure Using Multi-Attribute and Probabilistic Neural Network Techniques

First, the multiple attribute linear regression analysis has been performed for pore pressure prediction using five different external attributes. Every attribute has a different correlation coefficient with pore pressure and varying training errors. The analysis has been performed in time window of Basal Sand reservoir at well location of Naimat-Basal-01.

Figure 6.8 shows the list of attributes which are used in multi-attribute analysis with their training errors respectively.

Table 6.1 List of Multiple Attributes with training errors.

Sr no	Target	Final Attribute	Training Error (psi)
1	**Pressure**	**Amplitude Weighted Phase(Inverted_Zp)**	**24.1**
2	**Pressure**	**Amplitude Weighted Cosine Phase**	**23.4**
3	**Pressure**	**Cosine Instantaneous Phase**	**22.6**
4	**Pressure**	**Amplitude Envelope (Inverted_Zp)**	**21.9**
5	**Pressure**	**Instantaneous Frequency**	**21.8**

The correlation coefficient between actual well pore pressure and modelled/predicted pore pressure is 0.69 and the average error is 22.7 (psi) using multiple attribute linear regression analysis. The training result of multiple attribute regression analysis using five external attributes is shown above in Table 6.1. These results have been driven out by pointing those external attributes which are possessing low training errors while induced for the sake of pore pressure prediction. Every attribute have a distinct characteristic property resembling with target pore pressure variable.

The probabilistic neural network (PNN) is a non-linear approach and has been widely used for several years in geophysical studies. It is a non-linear interpolation technique using neural network implementation. It uses weighted distance approach between the sample points for the interpolation (Mahmood et al., 2017). The correlation coefficient between actual well pore pressure and predicted pore pressure is found to be 0.69 when Multi-Attribute linear regression approach is used and it is increased up to 0.88 in case of PNN shown in Figure 6.8 (a & b). There is a significant match between actual and modelled/predicted pore pressure compared to multiple attribute regression analysis.

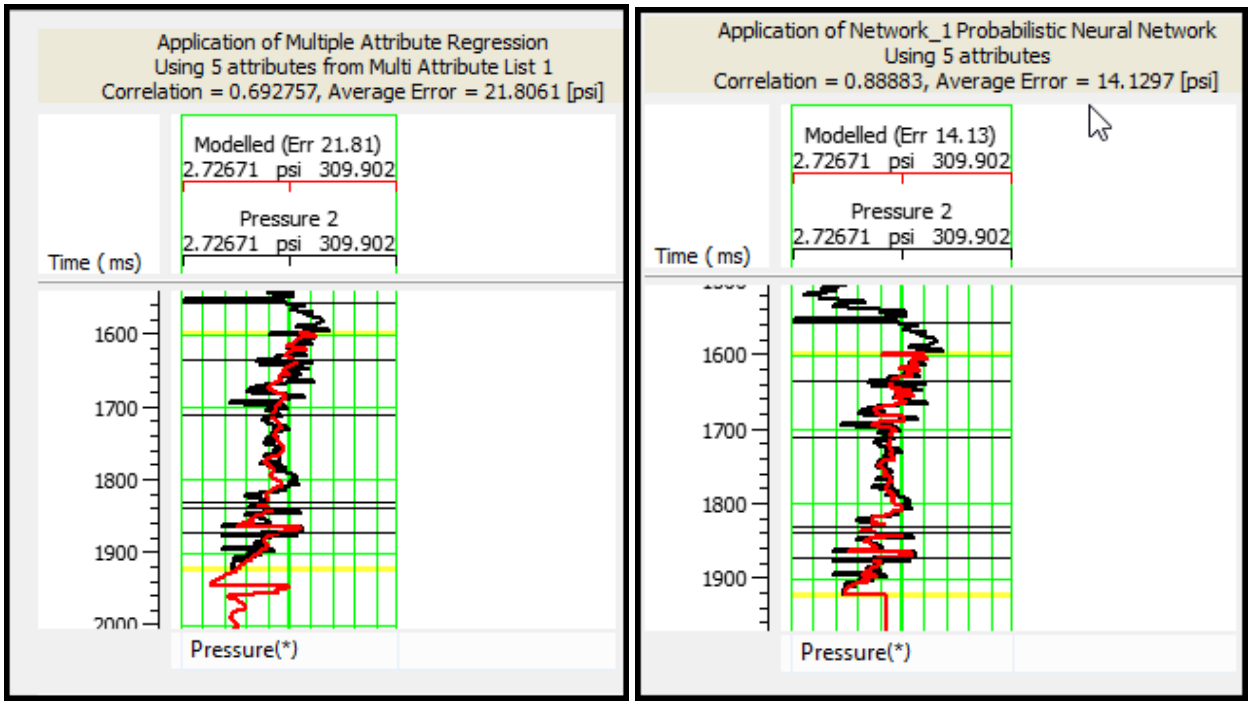

(a) (b)

Figure 6.8 (a) Training Result of Multiple Attribute Regression Analysis (b) Training result of probabilistic neural network.

This result will increased resolution in interpolation of pore pressure across entire line. Better the correlation coefficient between actual and predicted pore pressure, better will be the guidance power of seismically modelled pore pressure in extrapolation of actual well pore pressure. Figure 6.9 shows the cross-plot between actual pore pressure and modelled/predicted pore pressure on the basis of above training results.

The pore pressure predicted through probabilistic neural network exhibits an excellent correlation with the actual well point pore pressure. Final training result and cross-plot behavior is then implemented to the impedance section and inverted pore pressure section at line 2000KH-08 has been prepared as shown below in Figure 6.10. Impedance curve has been overlaid to cross-check the inverse behavior between pore pressure and impedance.

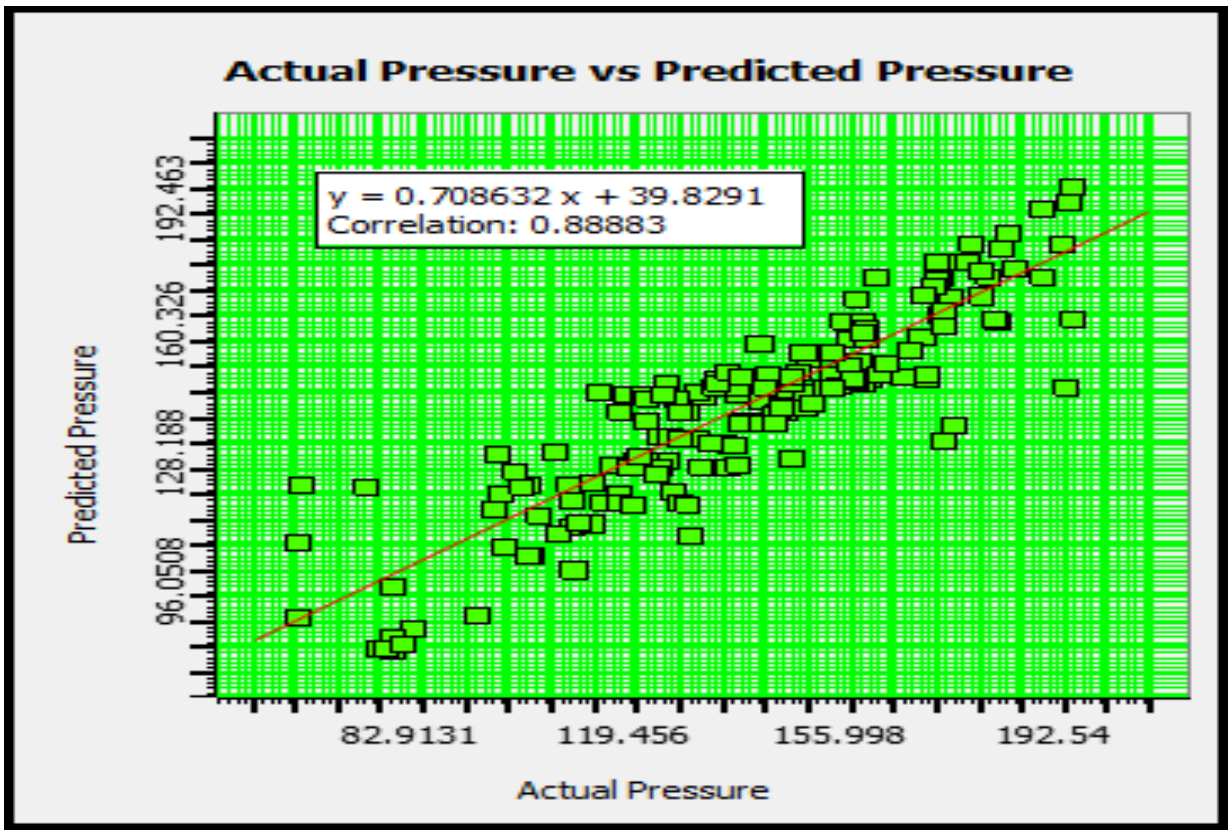

Figure 6.9 Cross-plot of actual and predicted porosity.

6.15 Magnitude of In Situ Stresses

To consider the ranges of stress magnitudes at depth in the different tectonic regime it is necessary to evaluate them in the context of the vertical stress and pore pressure. Because the prediction of horizontal stress depend upon the estimation of vertical stress. Supposing verticality of one component of the main stress; vertical boreholes are parallel to vertical stress (Sv). Therefore, SHmax and Shmin will be two other main stresses (Zhang, 2011).

6.15.1 Vertical Stress

As mentioned previously vertical stress or overburden can be calculated by integrating density log from surface to desired depth and can be calculate as:

$$Sv = \int_{Z2}^{Z1} p(z) g dz \qquad (6.10)$$

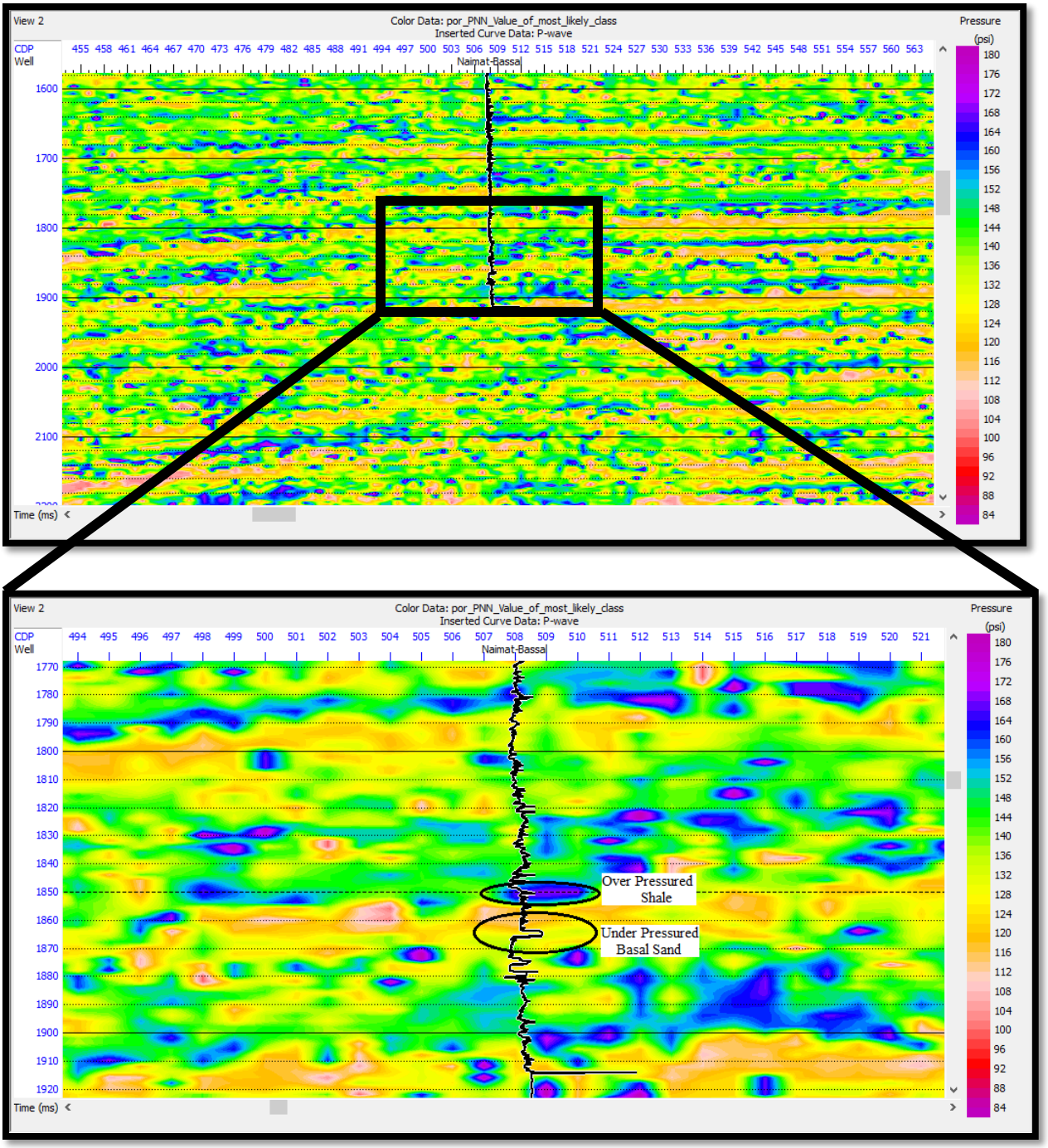

Figure 6.10 Extrapolation of predicted pore pressures for Naimat-Basal-01well on seismic line 2003KH-08 using seismic.

6.15.2 Minimum Horizontal Stress

Minimum horizontal stress or fracture pressure can be estimated using leak-oftests and from geophysical data. The minimum stress is the minimum principal in-situ stress and typically

equal to the fracture closure pressure, which can be observed on the decay of curve in a leak-off test following the breakdown pressure (Zhang, 2011). The minimum stress method, as shown in the following, is similar to the methods proposed by (Eaton (1969). In normal fault regime the horizontal stress can be estimated from Poisson ratio and vertical stress (Zhang, 2011).

6.15.3 Fracture Pressure and Closure Stress Ratio

Closure pressure or closure stress is defined as an analysis parameter used in hydraulic fracture design to indicate the pressure at which the fracture effectively closes without proppant in place'. In general it is empirically related to the minimum horizontal stress (Zoback, 2007). Basically it is the ratio of Poisson ratio and can be calculated from seismic and well data using Vp/Vs (v) ratio.

$$Closure\ stress\ ratio\ =\ v/(1-v) \tag{6.11}$$

Then the fracture pressure or minimum horizontal stress can be calculated as:

$$Shmin\ =\ v/(1-v)(Sv-pp)+pp+\Delta \tag{6.12}$$

The fracture pressure is the pressure which is required to fracture the formation which is equal to minimum horizontal stress. The accurate prediction of minimum horizontal stress is crucial in hydraulic fracturing and for shear failure prediction. The computed fracture gradient must be calibrated with leak-of-test. In order to calibrate the closure stress to actual measurements taken in the field, an additional term called the tectonic stress term (Delta in equation 6.12) is often required to be added to the closure stress equation thereby shifting the profile to match the measured values.

Figures 6.11 and 6.12 shows well based fracture gradient prediction for well Naimat-Basal-01 and Siraj-South-01. These fracture gradients was computed using equation 6.12. These computed minimum horizontal stresses was calibrated with LOT. As mentioned before this fracture gradient must be greater than pore pressure for sustaining well bore, which is greater throughout the well. For safe drilling the mud weight must be between pore pressure and fracture pressure.

The method used on well can be used to predict fracture pressure for whole survey using seismic data Fracture pressure profile can extract at any location for the drilling purpose.

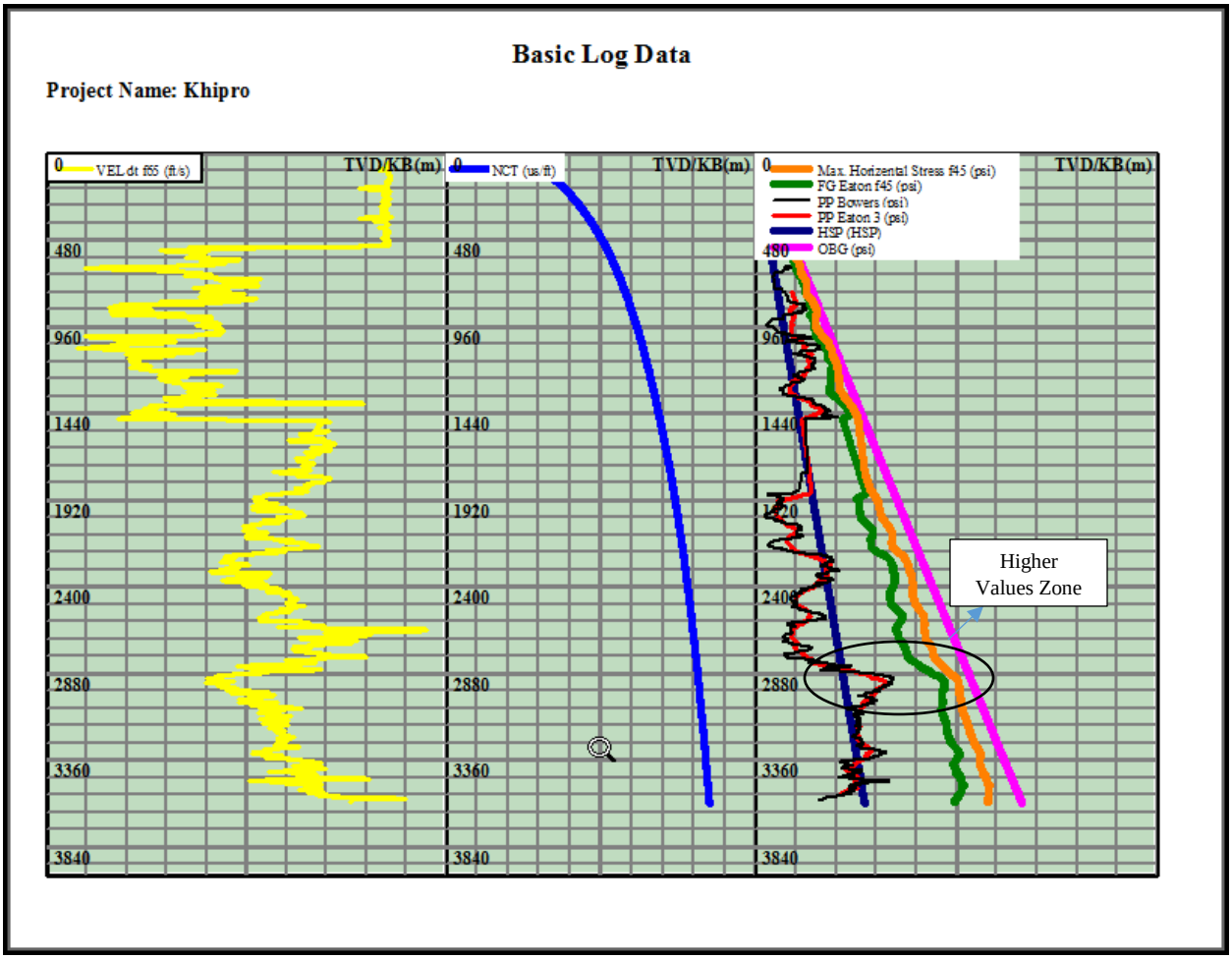

Figure 6.11 Fracture gradient or minimum horizontal stress along with maximum horizontal stress for Naimat-Basal-01 well.

6.15.4 Maximum Horizontal Stress

The maximum horizontal stress is always one of the major unknowns in the world of geomechanics as there is no straight way to measure it. This can be constrained either by using the severity of wellbore breakouts (Zoback, 2007) or by using advanced sonic measurements (Sayers et al. 2002). The magnitudes of the horizontal stresses are of the highest importance as the magnitudes with depth define the type of faulting regime that the formation of interest lies in.

The magnitude of the maximum horizontal stress can be estimated using other data, such as the tectonic regime, the magnitude of the minimum stress, and/or geological province or from well bore failure.

One empirical relation for calculating maximum horizontal stress is a ratio of the difference between the minimum stress and the overburden stress, using a horizontal stress increment factor, k given by equation as:

$$Shmax = Shmin + K * (Sv - Shmin) \quad (6.13)$$

A k value of 0.5 represents that the SHG is intermediate between the values of the minimum stress and the overburden stress. So it is important to determine the ordering of the principal stresses in the current stress regime. As study area is normal fault regime and according to Anderson's classification scheme $SHmax$ must be intermediate stress. Figure 6.11 and 6.12 shows well based minimum horizontal estimation, it can be seen that it is intermediate between overburden and maximum horizontal stress.

6.16 Relative Stress Magnitudes and Anderson's Classification Scheme

There are three types of principal stresses (S1, S2 and S3) that act in subsurface. Before classifying these stresses in earth crust it is useful to consider the magnitude of principal stresses in terms of greatest, intermediate and least principal stress. As we know we have one vertical stress (Sv) and two horizontal stresses (Shmin and SHmax) act in depth but there relative magnitude is different in different faulting regime. E. M. Anderson (1951) originally proposed the relative stress magnitude in an area characterize by normal, reverse or strike slip faulting. The relative magnitudes of the principal stresses are simply related to the faulting style currently active in a region. In normal faulting regime relative stress magnitudes are Sv > SH > Sh, in strike slip fault SH > Sv > Sh and in reverse faulting regime SH > Sh > Sv. The Anderson classification scheme also defines the horizontal principal stress magnitudes with respect to the vertical stress. The vertical stress Sv, is the maximum principal stress (S1) in normal faulting regimes, the intermediate principal stress (S2) in strike-slip regimes and the least principal stress (S3) in reverse faulting regimes. This classification and relative magnitude are important for characterizing stresses. Since our area is rift associated and interpretation of seismic data shows normal faulting environment so we have to classify the stresses accordingly which is it should be Sv > SH > Sh, and least principle stress should be greater than pore pressure. This can be seen in Figures 6.11 and 6.12.

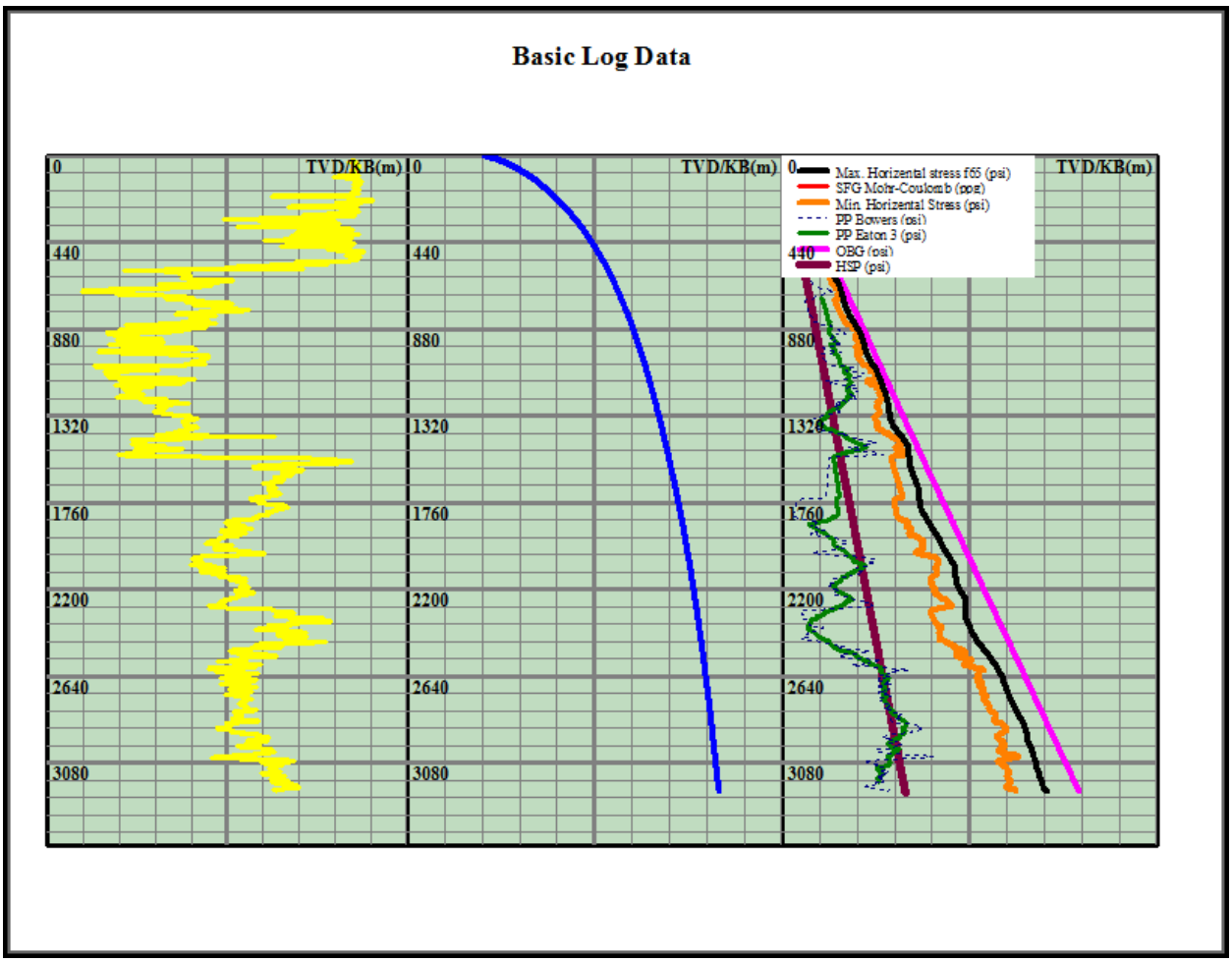

Figure 6.12 Fracture gradient or minimum horizontal stress along with maximum horizontal stress for Siraj-South-01 well.

Figures 6.11 and 6.12 shows the predicted fracture gradient for both the wells. Fracture is always created and propagated (grows) perpendicular to the least principal stress (minimum horizontal stress). Fracture orientation is influenced by various factors such as overburden pressure, pore pressure, tectonic forces, Poisson's ratio, Young's modulus, fracture toughness, and rock compressibility. It is extremely important to understand the principal stresses acting on the rock in the formation of interest for a successful fracture job. Engineers, petro physicists, geologists, and geoscientists are in charge of understanding and calculating the principal stresses.

Estimation of fracture gradient along with principal stresses and pore pressure is helpful in future if shales i.e. upper shale, lower shale or Talhar shale in studied area shows enough potential regarding hydrocarbon accumulation. Higher values of fracture gradient is indication of higher brittleness. In over pressured shale the values of Fracture gradient, Min. and Max. Horizontal stress

is also on higher side indicating the brittleness of shale is high as compared to sands in the area. The fracture gradient is the upper bound of the mud weight; therefore, the fracture gradient is an important parameter for mud weight design in both stages of drilling planning and operations. If the downhole mud weight is higher than the formation fracture gradient, then the wellbore will have tensile failures (i.e., the formation will be fractured), causing losses of drilling mud or even lost circulation (total losses of the mud). Therefore, fracture gradient prediction is directly related to drilling safety.

Conclusions

1. Interpretation of seismic data shows that the area is of extensional regime, with dominated normal faults which runs from deeper interval to the surface. At deeper and at reservoir interval the throw of fault is obvious but near surface it's dubious. The faults block according to interpretation are tilted and faults dip at range of 30-50^{o}.
2. Petro-physical estimates at reservoir level (Basal sand) shows good results i.e. effective porosities of range 8-15 % and Hydrocarbon saturation ranging 82-90%.
3. Estimated porosity using inversion technique shows the promising results along the line 2003KH-08 at Basal sand level
4. Prediction of pore pressure at Naimat-Basal-01 well highlighted the over pressured shale (seal rock) values ranging from 4000psi to 6200psi at depth of 2800m. Reservoir Basal sand is under pressured values ranging from 4000psi to 5000psi at a depth of 3500m. In Siraj-south-01 well over pressured sequences are not very much common.
5. Estimation of Pore pressure using Probabilistic neural network approach extrapolate the behavior of Pore pressure along the seismic line 2000KH-08. Correlation between estimated and actual Pore pressure is almost 88%.

References

- Ali, A., Alves, T. M., Saad, F. A., Ullah, M., Toqeer, M., and Hussain, M. (2018). Resource potential of gas reservoirs in South Pakistan and adjacent Indian subcontinent revealed by poststack inversion techniques. Journal of Natural Gas Science and Engineering, 49,41-55.
- Badley, M. E. (1985). Practical seismic interpretation by Michael E. Badley.
- Badley, M. E., and Gibson, B. (1987). Practical Seismic Interpretation by Michael E. Badley.
- Banks, C.J. and Warburton, J. (1986). Passive-Roof Duplex Geometry in the Frontal Structures of the Kirthar and Suleiman Mountain Belts, Pakistan. Journal of Structural Geology, 8, 229-237.
- Bowers, G. L. (1995). Pore pressure estimation from velocity data: Accounting for overpressure mechanisms besides undercompaction. SPE Drilling and Completion, 10(02), 89-95.
- Bruce, B., and Bowers, G. (2002). Pore pressure terminology. The Leading Edge, 21(2),170-173.
- Cannon, S. (2016). Petrophysics A Practical Guide. In Petrophysics A Practical Guide (p. 184).
- Chopra, S., and Huffman, A. R. (2006). Velocity determination for pore-pressure prediction. The Leading Edge, 25(12), 1502-1515.
- Cooke, D., and Cant, J. (2010). Model-based Seismic Inversion: Comparing deterministic and probabilistic approaches. CSEG Recorder, 28-39.
- Dickey, P. A., and Cox, W. C., (1977). Oil and gas reservoirs with subnormal pressures: AAPG Bulletin, v. 61, n. 12, p. 2134–2142.
- Dutta, N. C. (2002). Geopressure prediction using seismic data: Current status and the road ahead. Geophysics, 67(6), 2012-2041.
- Eaton, B. A. (1969). Fracture gradient prediction and its application in oilfield operations. Journal of petroleum technology, 21(10), 1-353.
- Eaton, B. A. (1972). The effect of overburden stress on geopressure prediction from well logs. Journal of Petroleum Technology, 24(08), 929-934.

- Gavotti, P. E. (2014). Model-based inversion of broadband seismic data (Doctoral dissertation, University of Calgary).
- Gadallah, M. R., and Fisher, R. (2009). Seismic Interpretation. In Exploration Geophysics, 149-221. Springer Berlin Heidelberg.
- Gibson, G. B. A. with C. R. (1982). Basic Well Log Analysis.pdf. In Basic Well Log Analysis.
- Harrold, T. W., Swarbrick, R. E., and Goulty, N. R. (1999). Pore pressure estimation from mudrock porosities in Tertiary basins, Southeast Asia. AAPG bulletin, 83(7), 1057-1067.
- Hermanrud, C., Wensaas, L., Teige, G. M. G., Bolas, H. N., Hansen, S., and Vik, E. (1998). Memoir 70, Chapter 4: Shale Porosities from Well Logs on Haltenbanken (Offshore Mid-Norway) Show No Influence of Overpressuring.
- Ibrahim, M., (2007). Seismic inversion Data, A tool for reservoir characterization/Modeling Sawan Gas Field - A case study, PAPG, ATC
- Jain, C. (2013). Effect of seismic wavelet phase on post stack inversion. 10th Biennial International Conference and exposition, 410.
- Kadri, I. B. (1995). Petroleum geology of Pakistan. Pakistan Petroleum Limited, 40-41.
- Kazmi, A.H. and Snee, L.W., (1989). Geology and Tectonics of Pakistan, 54-60.
- Kazmi, A.H., and Jan, M.Q., (1997). "Geology and Tectonics of Pakistan", Graphic Publishers, Karachi, Pakistan.
- Khan, A.M., Ahmed, R., Raza, H.A. and Kemal, A., (1986). Geology of petroleum in Kohat-Potwar depression, Pakistan. American Association of Petroleum Geologists, Bulletin 9, 44-51.
- Kneller, E., Ferrer, A., and Langlois, J. (2013). Benefits of broadband seismic data for reservoir characterization. In Santos Basin, Brasil: Thirteen International Congress of the Brazilian Geophysical Society, 966-970.
- Law, B. E., and Spencer, C. W. (1998). Memoir 70, Chapter 1: Abnormal Pressure in Hydrocarbon Environments.
- Mahmood, M.F., Shakir, U., Abuzar, M.K., Khan, M.A., Khattak, N.U., Hussain, H.S., Tahir, A.R., 2017. Probabilistic neural network approach for porosity prediction in

Balkassar area: A case study. J. Himal. Earth Sci. 50, 111–120.

- Nwankwo, C.N. and Kalu, S.O. (2016) Integrated Approach to Pore Pressure and Fracture Pressure Prediction Using Well Logs: Case Study of Onshore Niger-Delta Sedimentary Basin. Open Journal of Geology, 6, 1279-1295.
- Osborne, M. J., and Swarbrick, R. E. (1997). Mechanisms for generating overpressure in sedimentary basins: a reevaluation. AAPG bulletin, 81(6), 1023-1041.
- Orient Petroleum International Inc. (2009). Annual report, Sector G-10/4 Islamabad. Pakistan.
- Petro-consultants, (1996). Petroleum exploration and production digital database: Petro-consultants, Inc, Houston TX 77274-0619, U.S.A.
- Raza, H. A., Ahmed, R., and Ali, S. M. (1990). Pakistan offshore: an attractive frontier. Pakistan Journal of Hydrocarbon Research, 2(2), 1-42.
- Rider, M. H. (2002). The Geological Interpretation of Well Logs [Malcolm H. Rider] (2nd Ed.) .pdf. In The Geological Interpretation of Well Logs.
- Sayers, C. M., Johnson, G. M., and Denyer, G. (2002). Predrill pore-pressure prediction using seismic data. Geophysics, 67(4), 1286-1292.
- Sen, M.K. and Stoffa, P.L. (1995). Global optimization methods in geophysical inversion, The Netherlands: Elsevier Science Publications.
- Shah, S. M. I. (1977). Stratigraphy of Pakistan. Quetta, Pakistan: Director General, Geological Survey of Pakistan.
- Swarbrick, R. (2012). Review of pore-pressure prediction challenges in high-temperature areas. The Leading Edge, 31(11), 1288-1294.
- Swarbrick, R. E., Osborne, M. J., and Yardley, G. S. (2001). AAPG Memoir 76, Chapter 1: Comparison of Overpressure Magnitude Resulting from the Main Generating Mechanisms.
- Terzaghi, K. (1943). Theory of Consolidation, John Wiley and Sons, Inc 265-296.
- Tingay, M. R., Hillis, R. R., Swarbrick, R. E., Morley, C. K., and Damit, A. R. (2009).
- Veeken, P.C.H. and De Silva, M. 2004. Seismic inversion methods and some of their con-straints. First Break, 22:47-70.

- Wasimuddin, M., S.M.M. Alam and S.M.S. Ahmed., 2004. Studied Zaur Structure a Complex trap in a poor seismic data area. SPE. PAPG Annual Technical Conference, Islamabad, Pakistan. 146-124. Fair printing services, Karachi.
- Wikel, K., (2011). Geomechanics: bridging the gap from geophysics to engineering in unconventional reservoirs. First Break, 29, 71-80.
- Zaigham, N.A., and K.A. Mallick, (2000), Bela ophiolite zone of southern Pakistan: Tectonic setting and associated mineral deposits: GSA Bulletin, v.112, no. 3, 478-489.
- Zhang, J. (2011). Pore pressure prediction from well logs: Methods, modifications, and new approaches. Earth-Science Reviews, 108(1), 50-63.
- Zoback, M.D. (2007). Reservoir Geomechanics, Cambridge University Press, 449.